Biochemical and Biophysical Research Communications 405 (2011) 610–614

Contents lists available at ScienceDirect

Biochemical and Biophysical Research Communications

journal homepage: www.elsevier.com/locate/ybbrc

Limited expression of reticulocalbin-1 in lymphatic endothelial cells in lung tumor but not in normal lung

Yasunobu Yoshida [a,b,1], Takuya Yamashita [a,c,1], Kazuya Nagano [a,1], Sunao Imai [a], Hiromi Nabeshi [a,c], Tomoaki Yoshikawa [a,c], Yasuo Yoshioka [a,c,d], Yasuhiro Abe [a], Haruhiko Kamada [a,d], Yasuo Tsutsumi [a,c,d], Shin-ichi Tsunoda [a,b,d,*]

[a] Laboratory of Biopharmaceutical Research, National Institute of Biomedical Innovation, 7-6-8 Saito-Asagi, Ibaraki, Osaka 567-0085, Japan
[b] Department of Biomedical Innovation, Graduate School of Pharmaceutical Sciences, Osaka University, 1-6 Yamadaoka, Suita, Osaka 565-0871, Japan
[c] Department of Toxicology and Safety Science, Graduate School of Pharmaceutical Sciences, Osaka University, 1-6 Yamadaoka, Suita, Osaka 565-0871, Japan
[d] The Center of Advanced Medical Engineering and Informatics, Osaka University, 1-6 Yamadaoka, Suita, Osaka 565-0871, Japan

ARTICLE INFO

Article history:
Received 11 January 2011
Available online 25 January 2011

Keywords:
Tumor lymphatic endothelial cells
Lymph node metastasis
Proteomics
Reticulocalbin-1
Lung cancer

ABSTRACT

Lymphatic endothelial cells in tumors (T-LECs) are considered to have different characteristics from LECs in non-tumor tissues (N-LECs). However, differences between the two types have not been well analyzed at molecular level. In this report, we performed differential proteome analysis of T-LEC and N-LEC models prepared by cultivation of LECs in tumor conditioned medium. By expression profiling of identified proteins using tissue microarrays, reticulocalbin-1 was found to be expressed in clinical specimen-derived T-LECs and lung cancer cells but not N-LECs. It is suggested that reticulocalbin-1 may be an important molecule in understanding T-LEC function and control of lymphatic metastasis.

1. Introduction

Since lymph node metastasis in cancer is one of the most important prognostic factors, useful diagnostic and therapeutic methods for such pathology are highly desirable [1,2]. Blood vessel formation, or angiogenesis in tumors, is well known to be an essential contributor to tumor metastasis [3–5]. Various approaches have been reported in the study of tumor blood vessels, such as construction of *in vitro* tumor vascular endothelial cell models using conditioned medium (CM) from cancer cells [6–8]. In these studies, proteins highly expressed in tumor vascular endothelial cells have been identified (e.g. vascular endothelial growth factor receptor 2 (VEGFR2), tumor endothelial marker 7 (TEM7) and ROBO4) [9–13]. Moreover, an antibody drug to VEGF has already been used in the clinic [14,15]. As well as tumor blood vessels, lymphangiogenesis in tumors is also considered to be an important factor in lymphatic metastasis. However, the study of tumor lymphatic vessels is at an early stage. One of the reasons is that primary culture of LECs has only been established recently [16,17]. It has been reported that lymphatic vessels or lymphatic endothelial cells in tumors (T-LECs) have more invasive and neogenetic characteristics, which are distinct from those in normal tissues [18,19]. The difference in these characteristics suggests that molecules specific for tumor lymphatic vessels may be expressed. However, little is known about the molecular biology of tumor lymphatic vessels, in contrast to the situation with tumor vascular vessels [3–5]. Recently, proteome analysis has been undertaken, as one approach to the elucidation of events at molecular level, because proteins are the molecules which directly determine vital functions [20,21]. Consequently we focused on tumor lymphatic vessels and using proteome analysis, sought to identify tumor lymphatic endothelial cell (T-LECs)-related proteins to elucidate molecular mechanisms, with a view to development of molecular targeting therapeutic approaches.

In advancing the study according to this strategy, we had two problems. Firstly, it is not possible to collect sufficient amounts of sample, i.e. it is very difficult to isolate LECs from tumor tissues *in vivo* and obtain sufficient amounts for proteome analysis. Therefore, we firstly constructed a T-LEC model *in vitro* using CM from metastatic cancer cells. Because such CM includes various liquid factors produced from metastatic cancer cells, we considered it would appropriately mimic the environment in metastatic tumor tissues. The second problem relates to validation of identified proteins. Because many candidate proteins that are high- or

* Corresponding author at: Laboratory of Biopharmaceutical Research, National Institute of Biomedical Innovation, 7-6-8 Saito-Asagi, Ibaraki, Osaka 567-0085, Japan. Fax: +81 72 641 9817.
E-mail address: tsunoda@nibio.go.jp (S.-i. Tsunoda).
[1] These authors contributed equally to this work.

0006-291X/$ - see front matter © 2011 Elsevier Inc. All rights reserved.
doi:10.1016/j.bbrc.2011.01.077

low-expressed in diseased tissues are found by such a procedure, it is important to validate and focus on the appropriate proteins. Therefore we used a tissue microarray approach, employing a large number of normal tissues and tumor tissues and analyzing the relationship between protein expression and clinical information.

In this study, we searched for T-LEC-related proteins by two-dimensional differential in-gel electrophoresis (2D-DIGE) analysis using the T-LEC model, and validated the identified proteins as T-LEC-related by tissue microarray analysis.

2. Materials and methods

2.1. Cell lines

Primary normal human lung lymphatic microvascular endothelial cells (LECs) were purchased from Lonza Inc., (product name; HMVEC-LLy). LECs were confirmed to express the lymphatic markers CD31 and podoplanin in at least 95% of cells by flow cytometry. Cells were maintained at 37 °C in a humidified atmosphere of 5% CO_2 using an EGM-2-MV BulletKit (Lonza) and used in experiments within three passages after purchase. The human lung cancer cells line, RERF-LC-KJ, which is known to have high metastatic potential to lymphnode in immunodeficient mice [22], was purchased from the Japanese Collection of Research Bioresources (JCRB) cell bank and cultured in RPMI1640 supplemented with 10% FCS. Primary normal human bronchial epithelial (NHBE) cells were purchased from Lonza and were maintained using a BEGM BulletKit (Lonza).

2.2. Tumor and normal tissue lymphatic endothelial cell models

Conditioned medium (CM) was prepared from the supernatant of 48 h cultures of RERF-LC-KJ and NHBE cells. The collected supernatants were subsequently filtered (0.2 μm pores) to remove cellular debris. LECs were cultured in a medium containing 10% FCS and 50% tumor cells or NHBE cell CM for 48 h and used as models of lymphatic endothelial cells in tumor (T-LECs) and normal tissue (N-LECs), respectively.

2.3. In vitro tube formation assay

Twentyfour-well culture plates were coated with 300 μl of Matrigel basement membrane matrix (BD Bioscience) per well according to the manufacturer's instructions. LEC suspensions (250 μl), each containing 10% FCS and 50% of either CM, were seeded on the Matrigel-coated wells (3×10^4 cells/well). After incubation at 37 °C for 6 h, cells were stained with Calcein-AM solution (Dojindo Laboratories Co.) and images captured with a fluorescence microscope (Power IX81, Olympus). Tube formation of LECs was quantified as tube length per set of eight randomly selected fields per group using image analysis software (MetaXpress, Molecular Devices, Inc.,).

2.4. In vitro invasion assay

LECs were pre-cultured for 24 h in serum-free EBM-2 medium (Takara Bio). The membrane of 96-well chamber plates was coated with 50 μl of basement membrane extract (Cultrex) and dried overnight at 37 °C. LECs (5×10^4 cells per well) were added to the upper chambers and 150 μl of medium containing 10% FCS and 50% of either CM were added to the lower chambers. After incubation for 48 h at 37 °C, the non-invasive cells on the upper side of the membranes were removed by scrubbing. The invasive cells in the lower chambers were quantified by staining with Calcein-AM solution and a fluorescence microplate reader.

2.5. 2D-DIGE analysis

Proteome analysis was performed by 2D-DIGE and mass spectrometry. LECs cultured in CM of RERF-LC-KJ cells and NHBE cells for 48 h were solubilized with 7 M urea, 2 M thiourea, 4% CHAPS and 10 mM Tris–HCl (pH 8.5). The lysates from each LEC type were purified using a 2D-Clean up kit (GE Healthcare Biosciences) and labeled with Cy3 or Cy5 protein-labeling dye (GE Healthcare Biosciences) at a ratio of 50 μg protein: 400 pmol dye according to the manufacturer's instructions. For the first isoelectric focusing separation by 2D-electrophoresis, 50 μg of each labeled sample was mixed with rehydration buffer (7 M urea, 2 M thiourea, 4% CHAPS, 2% DTT, 2% Pharmalyte (GE Healthcare Biosciences)) and applied to a 24-cm immobilized pH gradient gel strip (IPG-strip pH 4–7 NL, GE Healthcare Biosciences). The samples for the spot-picking gel were prepared without Cy-dye labelling. For the second dimension separation, the IPG-strips were applied to SDS–PAGE gels (10% polyacrylamide and 2.7% *N,N′*-diallyltartardiamide). After electrophoresis, the gels were scanned with a fluoroimager (Typhoon Trio, GE Healthcare Biosciences). The spot-picking gel was also scanned after staining with Flamingo solution (Bio-Rad). Quantitative analysis of protein spots was carried out with Decyder-DIA software (GE Healthcare Biosciences). Protein spots of differential expression were picked using an Ettan Spot Picker (GE Healthcare Biosciences).

2.6. In-gel tryptic digestion

The picked gel pieces were twice destained with 50% acetonitrile/50 mM NH_4HCO_3 for 20 min, dehydrated with 75% acetonitrile for 20 min, and then dried using a centrifugal concentrator. Next, 5 μl of 20 μl/ml mass spectrometry grade trypsin solution (Promega) was added to each gel piece and incubated for 16 h at 37 °C. To extract the resulting peptides from the gel pieces, they were treated with a series of acetonitrile/trifluoroacetic acid (TFA) solution. First, 50 μl of 50% (v/v) acetonitrile in 1% (v/v) aqueous TFA was added to the gel pieces, which were then sonicated for 5 min. Next, the solution was collected and 80% (v/v) acetonitrile in 0.2% TFA added. Finally, 100% acetonitrile was added for the last extraction. The peptides were dried and then resuspended in 10 μl of 0.1% TFA before being cleaned, using ZipTip™ μC_{18} pipette tips (Millipore). The tips were wetted with three washes in 50% acetonitrile and equilibrated with three washes in 0.1% TFA, then the peptides were aspirated 10 times to ensure binding to the column. The column and peptides were washed three times in 0.1% TFA before being eluted in 1 μl of 80% acetonitrile/0.2% TFA.

2.7. Protein identification by mass spectrometry

The tryptic digests (0.6 μl) were mixed with 0.6 μl α-cyano-4-hydroxy-trans-cinnamic acid saturated in a 0.1% TFA and acetonitrile (1:1 vol/vol). Each mixture was deposited onto the well of a target plate and then analyzed by matrix-assisted laser desorption ionization time-of-flight mass spectrometry (AutoflexII, Bruker Daltonics). The Mascot search engine (Matrixscience) was initially used to query the entire theoretical tryptic peptide as well as the SwissProt protein sequence database.

2.8. Tissue microarray analysis

Human lung cancer and normal tissue microarrays (Biomax) were deparaffinated in xylene and rehydrated in a graded series of ethanol concentrations. Heat-induced epitope retrieval was performed while maintaining the Target Retrieval Solution (pH 9, Dako) at the desired temperature according to the manufacturer's instructions. After heat-induced epitope retrieval treatment,

endogenous peroxidase was blocked with 0.3% H_2O_2 in TBS for 5 min followed by washing twice in TBS. After blocking with 5% BSA solution, the slides were incubated for 60 min with the following antibodies: anti-podoplanin (Dako), anti- HYOU-1 (Abnova), anti-hnRNPK (Abcam), anti-GRIM-12 (Affinity BioReagents) anti-vimentin (Abcam) and anti-reticulocalbin-1 (Novus Biologicals). After washing with the wash buffer (Dako), each array was stained with Envision + Dual Link (DAKO) and 3, 3′-diaminobenzidine. After development, arrays were lightly counterstained with Mayer's hematoxylin, and mounted with resinous mounting medium. All procedures were performed using AutoStainer (Dako).

2.9. Tissue microarray scoring

The optimized staining condition for lung tumor microarray was determined based on the coexistence of both positive and negative cells in the same tissue sample. Stain was considered positive when reaction products were localized in the expected cellular component. The criteria for evaluation were as follows: distribution score was scored as 0 (0%), 1 (1–50%), and 2 (51–100%) to indicate the percentage of positive cells in all tumor cells present in one tissue. The intensity of the stain (intensity score) was scored as 0 (no signal), 1 (weak), 2 (moderate), and 3 (marked). The sum of distribution score and intensity score was then calculated as a total score (TS) of TS0 (sum = 0), TS1 (sum = 2), TS2 (sum = 3), and TS3 (sum = 4–5). Throughout this study, TS0 or TS1 was regarded as negative, whereas TS2 or TS3 was regarded as positive.

3. Results

3.1. Evaluation of T-LEC model

In order to confirm that the *in vitro* tumor lymphatic vessel model reflected properties of *in vivo* tumor lymphatic vessels, tube formation and invasiveness were examined. The tube formation assay showed that the tube length of LECs in the RERF-LC-KJ CM group was significantly greater than that in the normal cell CM group (Fig. 1A). The invasion assay showed that the number of invasive LECs in the RERF-LC-KJ CM group was also significantly greater than that in the normal CM group (Fig. 1B). No difference between groups was observed in cell proliferation (data not shown). These data suggested that the *in vitro* T-LEC model using CM reflected properties of *in vivo* tumor lymphatic vessels, at least as regards enhanced lymphangiogenesis.

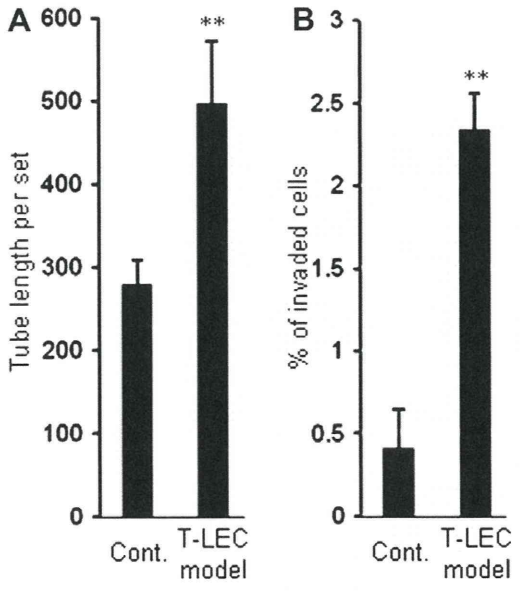

Fig. 1. Enhancement of lymphangiogenesis by treatment with CM of metastatic lung cancer cells. Effect on lymphangiogenesis of treatment with CM from the metastatic lung cancer RERF-LC-KJ cell line was assessed by (A) tube formation assay and (B) invasion assay. Error bars indicate the mean ± S.D. of triplicate assays (**$P < 0.01$).

3.2. Differential proteome analysis in T-LEC and N-LEC models

In order to search for T-LEC-related proteins, we performed differential proteome analysis of the T-LEC and N-LEC models (Fig. 2). By quantitative image analysis, protein spots representing >1.5-fold alteration in expression were found and identified by mass spectrometry (Table 1).

3.3. Validation of the candidate proteins using tissue microarrays

In order to validate the identified proteins as T-LEC-related proteins, we analyzed their expression profile using the lymphatic vessel tissue microarray in lung tumor and normal lung tissues. Results showed that heterogeneous nuclear ribonucleoprotein K (hnRNPK), gene associated with retinoid interferon-induced mortality 12 (GRIM-12) and vimentin were expressed both in T-LECs and N-LECs. In contrast, hypoxia up-regulated protein 1 (HYOU1) was expressed in neither T-LECs nor N-LECs (data not shown). Interestingly, reticulocalbin-1 was specifically expressed in T-LECs, while podoplanin, a recognized lymphatic vessel marker, was expressed in all T-LECs and N-LECs (Fig. 3). Moreover, the expression profiles of these molecules in lung cancer tissues and normal lung tissues were analyzed (Table 2). The result from tissue microarray analysis showed that GRIM-12 and vimentin were expressed in normal lung and tumor tissues. On the other hand, HYOU1 was specifically expressed in approximately 40% of lung cancer patients, while hnRNPK and reticulocalbin-1 were expressed in approximately 70% of such patients.

4. Discussion

This paper is the first report demonstrating differential proteome analysis of T-LEC and N-LEC models using CM of metastatic lung cancer cells and normal cells. We first found that the T-LEC model, obtained from LECs cultured in CM of metastatic cancer

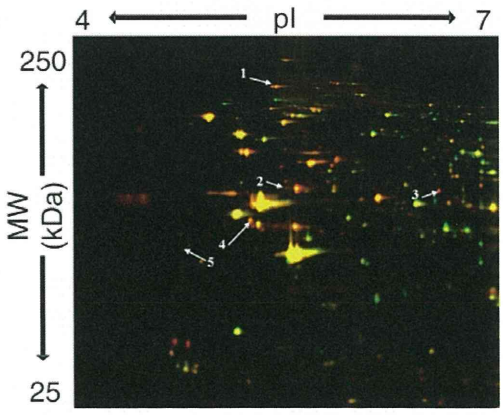

Fig. 2. 2D-DIGE image of fluorescently labeled LEC proteins cultured in CM of metastatic lung cancer cells and normal bronchial epithelial cells. Proteins prepared from LEC cultured in CM from the metastatic lung cancer RERF-LC-KJ cell line, and from normal bronchial epithelial cells (NHBE), were labeled with Cy3 and Cy5, and used for 2D-DIGE analysis. The spots indicated by arrows show the proteins identified by MALDI-TOF/MS.

Table 1
Identification of differentially-expressed proteins in T-LEC model by MALDI-TOF/MS.

Spot	Protein name	Accession No.	MW (kDa)	pI	Expression ratio (fold) [Cancer CM/Normal CM]
#1	HYOU1	Q9Y4L1	111	5.2	1.7
#2	hnRNPK	P61978	48	5.5	2.0
#3	GRIM-12	Q16881	55	6.4	1.8
#4	Vimentin	P08670	54	5.1	1.9
#5	Reticulocalbin-1	Q15293	39	4.9	1.9

Table 2
Positive rate of identified proteins in lung cancer and normal lung tissues.

Protein name	Positive rate of identified proteins			
	Normal lung tissues		Lung cancer tissues	
Podoplanin	11/29 cases	(38%)	70/221 cases	(32%)
HYOU1	0/29 cases	(0%)	87/221 cases	(39%)
hnRNPK	0/29 cases	(0%)	153/221 cases	(69%)
GRIM-12	3/29 cases	(10%)	114/221 cases	(52%)
Vimentin	15/29 cases	(52%)	90/221 cases	(41%)
Reticulocalbin-1	0/29 cases	(0%)	158/221 cases	(72%)

cells, was a useful example to use in searching for candidate tumor lymphatic endothelial cell markers, since it showed more invasive and neogenetic characteristics than that of normal cells in *in vitro* experiments. Since induction of vascular angiogenesis in tumors serves to provide nutrients, lymphangiogenesis induction in tumors is considered to facilitate removal of waste material. Thelen has reported that higher levels of lymphatic vessel density were related to a higher degree of metastasis, by statistical analysis of clinical specimens [23]. This report suggests that lymphatic endothelial cells in metastatic tumors are probably activated and induce their migration *via* soluble factors obtained from the tumor cells. The T-LEC model used in our experiments is considered to be activated by CM from metastatic tumor cells.

Using the T-LEC and N-LEC models, we performed differential proteome analysis to search for marker proteins expressed on T-LECs and identified a candidate protein reticulocalbin-1. Although lymphatic vessel endothelial hyaluronic acid receptor-1 (Lyve-1), podoplanin and vascular endothelial growth factor receptor-3 (VEGFR3) are known as lymphatic markers, these markers do not show specificity for T-LECs [24–26]. Interestingly, reticulocalbin-1 is shown to be expressed in T-LECs, but not N-LECs by TMA analysis. Reticulocalbin-1 is a member of the family of Ca^{2+}-binding proteins localized in the endoplasmic reticulum and is suggested to function in the secretory pathway of cells [27,28]. It is also reported that malignancy of hepatocellular carcinoma cell lines is increased by over-expression of reticulocalbin-1 [29]. Furthermore, a highly invasive mammary cancer cell line has been shown to express reticulocalbin-1, while a poorly invasive cancer cell line did not [30]. Thus, reticulocalbin-1 may be involved in invasion of lymphatic vessels into tumor tissues.

Since the identified proteins were validated using TMAs from many clinical specimens of lung cancer cases and normal tissues, we were able to identify the several candidates specifically expressed in lung cancer cells, namely HYOU1, hnRNPK and reticulocalbin-1. HYOU1 is induced by hypoxia and has a pivotal role in cytoprotective cellular mechanisms triggered by oxygen deprivation [31]. hnRNPK is a conserved RNA-binding protein that is involved in multiple processes of gene expression, including chromatin remodeling, transcription, and mRNA splicing, translation, and stability [32,33]. Recently HYOU1 expression in breast and colorectal cancer, and hnRNPK expression in breast cancer have been reported [34–36]. However, the relevance of these proteins to lung cancer has not been reported. Our data suggest that these proteins could be diagnostic and therapeutic targets in lung cancer. Furthermore, reticulocalbin-1 was highly expressed in lung tumor tissues compared to normal lung tissues, as well as being highly expressed in T-LECs compared to N-LECs. In addition, reticulocalbin-1 is reported to be expressed on cell membranes of some cancer cells [37]. Consequently, it could be a useful target for antibody therapy in cancer metastasis, at least in terms of expression profile. Further work is required to reveal the functions of these proteins in lung cancer.

In conclusion, we have identified reticulocalbin-1 as candidate T-LEC-related protein in lung tumors for the first time. Furthermore we have shown that HYOU1 and hnRNPK as highly expressed in lung tumors, by differential proteome analysis of the T-LEC model using CM. We hope that identified T-LEC-related proteins will contribute to advances in molecular biology and the development of diagnostic and therapeutic methods.

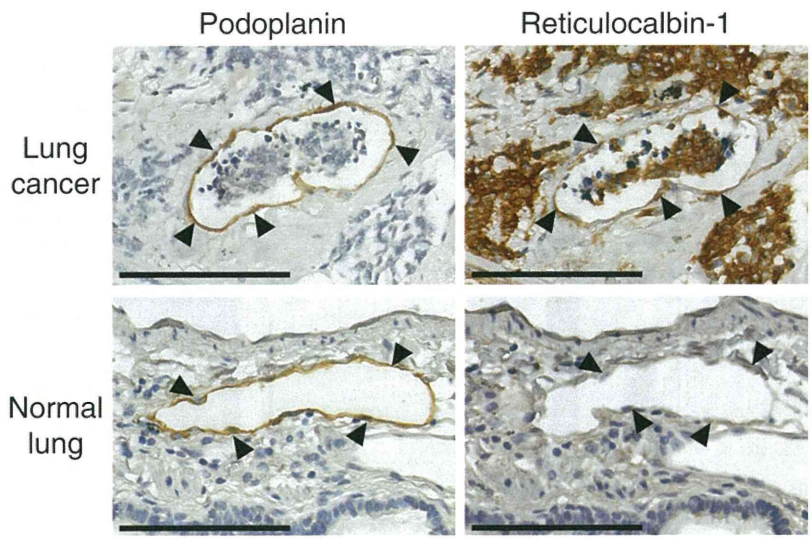

Fig. 3. Immunohistochemical staining of lymphatic vessels in human lung cancer and normal lung tissues using anti-podoplanin and anti-reticulocalbin-1 antibodies. Lymphatic vessels in human lung cancer and normal lung tissues were immunostained with anti-podoplanin and anti-reticulocalbin-1 antibodies and counter-stained by hematoxylin. The arrowheads indicate lymphatic endothelial cells. Scale bar is 100 μm.

Acknowledgments

This study was supported in part by Grants-in-Aid for Scientific Research from the Ministry of Education, Culture, Sports, Science and Technology of Japan, and from the Japan Society for the Promotion of Science (JSPS). This study was also supported in part by Health Labor Sciences Research Grants from the Ministry of Health, Labor and Welfare of Japan and by Health Sciences Research Grants for Research on Publicly Essential Drugs and Medical Devices from the Japan Health Sciences Foundation. The study sponsors had no part in study design or the writing of the manuscript.

References

[1] F. Celikoglu, S.I. Celikoglu, E.P. Goldberg, Intratumoural chemotherapy of lung cancer for diagnosis and treatment of draining lymph node metastasis, J. Pharm. Pharmacol. 62 (2010) 287–295.
[2] M.N. Elsheikh, A. Rinaldo, H. Hamakawa, M.E. Mahfouz, J.P. Rodrigo, J. Brennan, K.O. Devaney, J.R. Grandis, A. Ferlito, Importance of molecular analysis in detecting cervical lymph node metastasis in head and neck squamous cell carcinoma, Head Neck 28 (2006) 842–849.
[3] H. Konno, T. Tanaka, M. Baba, T. Kanai, S. Nakamura, Antiangiogenic therapy for liver metastasis of gastrointestinal malignancies, J. Hepatobiliary Pancreat. Surg. 6 (1999) 1–6.
[4] L.A. Liotta, P.S. Steeg, W.G. Stetler-Stevenson, Cancer metastasis and angiogenesis: an imbalance of positive and negative regulation, Cell 64 (1991) 327–336.
[5] V. Mahadevan, I.R. Hart, Metastasis and angiogenesis, Acta Oncol. 29 (1990) 97–103.
[6] P.J. Hepburn, K. Griffiths, M.E. Harper, Angiogenic factors expressed by human prostatic cell lines: effect on endothelial cell growth *in vitro*, Prostate 33 (1997) 123–132.
[7] A. Li, H. Li, J. Zhang, G. Jin, R. Xiu, The mitogenic and anti-apoptotic activity of tumor conditioned medium on endothelium, Clin. Hemorheol. Microcirc. 29 (2003) 375–382.
[8] Q.R. Yang, R.M. Smets, A. Neetens, D. Vanden Berghe, Human retinal pigment epithelial cells from different donors continuously produce a vascular endothelial cell-stimulating factor into serum-free medium, J. Cell Sci. 104 (Pt 1) (1993) 211–218.
[9] E.B. Carson-Walter, D.N. Watkins, A. Nanda, B. Vogelstein, K.W. Kinzler, B. St Croix, Cell surface tumor endothelial markers are conserved in mice and humans, Cancer Res. 61 (2001) 6649–6655.
[10] B. Fuchs, E. Mahlum, C. Halder, A. Maran, M. Yaszemski, B. Bode, M. Bolander, G. Sarkar, High expression of tumor endothelial marker 7 is associated with metastasis and poor survival of patients with osteogenic sarcoma, Gene 399 (2007) 137–143.
[11] L. Huminiecki, M. Gorn, S. Suchting, R. Poulsom, R. Bicknell, Magic roundabout is a new member of the roundabout receptor family that is endothelial specific and expressed at sites of active angiogenesis, Genomics 79 (2002) 547–552.
[12] B.I. Terman, M. Dougher-Vermazen, M.E. Carrion, D. Dimitrov, D.C. Armellino, D. Gospodarowicz, P. Bohlen, Identification of the KDR tyrosine kinase as a receptor for vascular endothelial cell growth factor, Biochem. Biophys. Res. Commun. 187 (1992) 1579–1586.
[13] Y. Yamaji, S. Yoshida, K. Ishikawa, A. Sengoku, K. Sato, A. Yoshida, R. Kuwahara, K. Ohuchida, E. Oki, H. Enaida, K. Fujisawa, T. Kono, T. Ishibashi, TEM7 (PLXDC1) in neovascular endothelial cells of fibrovascular membranes from patients with proliferative diabetic retinopathy, Invest. Ophthalmol. Vis. Sci. 49 (2008) 3151–3157.
[14] H.X. Chen, R.E. Gore-Langton, B.D. Cheson, Clinical trials referral resource: current clinical trials of the anti-VEGF monoclonal antibody bevacizumab, Oncology (Williston Park) 15 (2001) 1017, 1020, 1023–6.
[15] S. Shinkaruk, M. Bayle, G. Lain, G. Deleris, Vascular endothelial cell growth factor (VEGF), an emerging target for cancer chemotherapy, Curr. Med. Chem. Anticancer Agents 3 (2003) 95–117.
[16] M. Djoneidi, P. Brodt, Isolation and characterization of rat lymphatic endothelial cells, Microcirc. Endothelium Lymphatics 7 (1991) 161–182.
[17] L.V. Leak, M. Jones, Lymphangiogenesis *in vitro*: formation of lymphatic capillary-like channels from confluent monolayers of lymphatic endothelial cells, In Vitro Cell Dev. Biol. Anim. 30A (1994) 512–518.
[18] J.F. Donoghue, F.L. Lederman, B.J. Susil, P.A. Rogers, Lymphangiogenesis of normal endometrium and endometrial adenocarcinoma, Hum. Reprod. 22 (2007) 1705–1713.
[19] T. Omachi, Y. Kawai, R. Mizuno, T. Nomiyama, S. Miyagawa, T. Ohhashi, J. Nakayama, Immunohistochemical demonstration of proliferating lymphatic vessels in colorectal carcinoma and its clinicopathological significance, Cancer Lett. 246 (2007) 167–172.
[20] S. Hanash, Disease proteomics, Nature 422 (2003) 226–232.
[21] M.J. Page, B. Amess, C. Rohlff, C. Stubberfield, R. Parekh, Proteomics: a major new technology for the drug discovery process, Drug Discov. Today 4 (1999) 55–62.
[22] S. Teraoka, S. Kyoizumi, T. Seyama, M. Yamakido, M. Akiyama, A novel SCID mouse model for studying spontaneous metastasis of human lung cancer to human tissue, Jpn. J. Cancer Res. 86 (1995) 419–423.
[23] A. Thelen, A. Scholz, C. Benckert, W. Weichert, E. Dietz, B. Wiedenmann, P. Neuhaus, S. Jonas, Tumor-associated lymphangiogenesis correlates with lymph node metastases and prognosis in hilar cholangiocarcinoma, Ann. Surg. Oncol. 15 (2008) 791–799.
[24] S. Breiteneder-Geleff, A. Soleiman, H. Kowalski, R. Horvat, G. Amann, E. Kriehuber, K. Diem, W. Weninger, E. Tschachler, K. Alitalo, D. Kerjaschki, Angiosarcomas express mixed endothelial phenotypes of blood and lymphatic capillaries: podoplanin as a specific marker for lymphatic endothelium, Am. J. Pathol. 154 (1999) 385–394.
[25] A. Kaipainen, J. Korhonen, T. Mustonen, V.W. van Hinsbergh, G.H. Fang, D. Dumont, M. Breitman, K. Alitalo, Expression of the fms-like tyrosine kinase 4 gene becomes restricted to lymphatic endothelium during development, Proc. Natl. Acad. Sci. USA 92 (1995) 3566–3570.
[26] L. Trojan, M.S. Michel, F. Rensch, D.G. Jackson, P. Alken, R. Grobholz, Lymph and blood vessel architecture in benign and malignant prostatic tissue: lack of lymphangiogenesis in prostate carcinoma assessed with novel lymphatic marker lymphatic vessel endothelial hyaluronan receptor (LYVE-1), J. Urol. 172 (2004) 103–107.
[27] M. Ozawa, Cloning of a human homologue of mouse reticulocalbin reveals conservation of structural domains in the novel endoplasmic reticulum resident Ca(2+)-binding protein with multiple EF-hand motifs, J. Biochem. 117 (1995) 1113–1119.
[28] M. Ozawa, T. Muramatsu, Reticulocalbin, a novel endoplasmic reticulum resident Ca(2+)-binding protein with multiple EF-hand motifs and a carboxyl-terminal HDEL sequence, J. Biol. Chem. 268 (1993) 699–705.
[29] L.R. Yu, R. Zeng, X.X. Shao, N. Wang, Y.H. Xu, Q.C. Xia, Identification of differentially expressed proteins between human hepatoma and normal liver cell lines by two-dimensional electrophoresis and liquid chromatography-ion trap mass spectrometry, Electrophoresis 21 (2000) 3058–3068.
[30] Z. Liu, M.G. Brattain, H. Appert, Differential display of reticulocalbin in the highly invasive cell line, MDA-MB-435, versus the poorly invasive cell line, MCF-7, Biochem. Biophys. Res. Commun. 231 (1997) 283–289.
[31] K. Ozawa, K. Kuwabara, M. Tamatani, K. Takatsuji, Y. Tsukamoto, S. Kaneda, H. Yanagi, D.M. Stern, Y. Eguchi, Y. Tsujimoto, S. Ogawa, M. Tohyama, 150-kDa oxygen-regulated protein (ORP150) suppresses hypoxia-induced apoptotic cell death, J. Biol. Chem. 274 (1999) 6397–6404.
[32] C. Gaillard, E. Cabannes, F. Strauss, Identity of the RNA-binding protein K of hnRNP particles with protein H16, a sequence-specific single strand DNA-binding protein, Nucleic Acids Res. 22 (1994) 4183–4186.
[33] J. Ostrowski, K. Klimek-Tomczak, L.S. Wyrwicz, M. Mikula, D.S. Schullery, K. Bomsztyk, Heterogeneous nuclear ribonucleoprotein K enhances insulin-induced expression of mitochondrial UCP2 protein, J. Biol. Chem. 279 (2004) 54599–54609.
[34] A. Stojadinovic, J.A. Hooke, C.D. Shriver, A. Nissan, A.J. Kovatich, T.C. Kao, S. Ponniah, G.E. Peoples, M. Moroni, HYOU1/Orp150 expression in breast cancer, Med. Sci. Monit 13 (2007) BR231–239.
[35] O. Slaby, K. Sobkova, M. Svoboda, I. Garajova, P. Fabian, R. Hrstka, R. Nenutil, M. Sachlova, I. Kocakova, J. Michalek, T. Smerdova, D. Knoflickova, R. Vyzula, Significant over expression of Hsp110 gene during colorectal cancer progression, Oncol. Rep. 21 (2009) 1235–1241.
[36] B. Hamrita, K. Chahed, M. Kabbage, C.L. Guillier, M. Trimeche, A. Chaieb, L. Chouchane, Identification of tumor antigens that elicit a humoral immune response in breast cancer patients' sera by serological proteome analysis (SERPA), Clin. Chim. Acta 393 (2008) 95–102.
[37] C.R. Cooper, B. Graves, F. Pruitt, H. Chaib, J.E. Lynch, A.K. Cox, L. Sequeria, K.L. van Golen, A. Evans, K. Czymmek, R.S. Bullard, C.D. Donald, K. Sol-Church, J.D. Gendernalik, B. Weksler, M.C. Farach-Carson, J.A. Macoska, R.A. Sikes, K.J. Pienta, Novel surface expression of reticulocalbin 1 on bone endothelial cells and human prostate cancer cells is regulated by TNF-alpha, J. Cell Biochem. 104 (2008) 2298–2309.

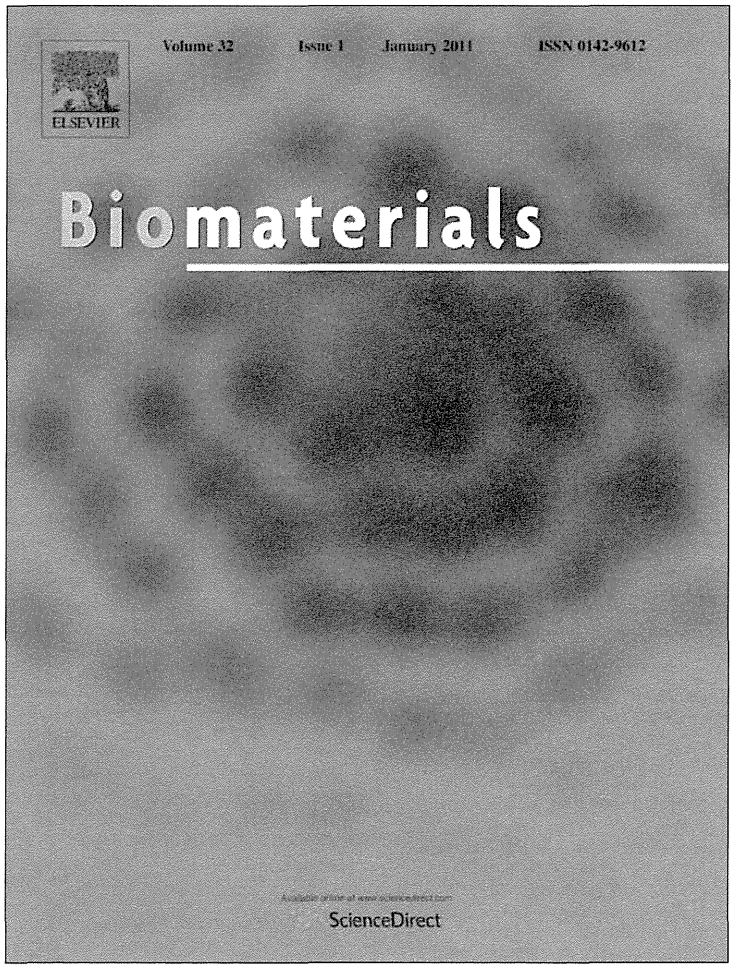

Biomaterials 32 (2011) 162–169

Contents lists available at ScienceDirect

Biomaterials

journal homepage: www.elsevier.com/locate/biomaterials

Development of an antibody proteomics system using a phage antibody library for efficient screening of biomarker proteins

Sunao Imai [a,1], Kazuya Nagano [a,1], Yasunobu Yoshida [a], Takayuki Okamura [a], Takuya Yamashita [a,b], Yasuhiro Abe [a], Tomoaki Yoshikawa [a,b], Yasuo Yoshioka [a,b,c], Haruhiko Kamada [a,c], Yohei Mukai [a,b], Shinsaku Nakagawa [b,c], Yasuo Tsutsumi [a,b,c], Shin-ichi Tsunoda [a,b,c,*]

[a] Laboratory of Biopharmaceutical Research, National Institute of Biomedical Innovation, 7-6-8 Saito-Asagi, Ibaraki, Osaka 567-0085, Japan
[b] Graduate School of Pharmaceutical Sciences, Osaka University, 1-6 Yamadaoka, Suita, Osaka 565-0871, Japan
[c] The Center of Advanced Medical Engineering and informatics, Osaka University, 1-6 Yamadaoka, Suita, Osaka 565-0871, Japan

ARTICLE INFO

Article history:
Received 27 August 2010
Accepted 14 September 2010
Available online 8 October 2010

Keywords:
Protein
Image analysis
Immunochemistry
Molecular biology
Antibody
Cancer

ABSTRACT

Proteomics-based analysis is currently the most promising approach for identifying biomarker proteins for use in drug development. However, many candidate biomarker proteins that are over- or under-expressed in diseased tissues are found by such a procedure. Thus, establishment of an efficient method for screening and validating the more valuable targets is urgently required. Here, we describe the development of an "antibody proteomics system" that facilitates the screening of biomarker proteins from many candidates by rapid preparation of cross-reacting antibodies using phage antibody library technology. Using two-dimensional differential in-gel electrophoresis analysis, 16 over-expressed proteins from breast cancer cells were identified. Specifically, proteins were recovered from the gel pieces and a portion of each sample was used for mass spectrometry analysis. The remainder was immobilized onto a nitrocellulose membrane for antibody-expressing phage enrichment and selection. Using this procedure, antibody-expressing phages against each protein were successfully isolated within two weeks. The expression profiles of the identified proteins were then acquired by immunostaining of breast tumor tissue microarrays with the antibody-expressing phages. Using this approach, expression of Eph receptor A10, TRAIL-R2 and Cytokeratin 8 in breast tumor tissues were successfully validated.

These results demonstrate the antibody proteomics system is an efficient method for screening tumor-related biomarker proteins.

1. Introduction

Proteomics-based analysis is the most promising approach for identifying tumor-related biomarker proteins used in the drug development process [1–3]. The technological development of proteomics to seek and identify differentially expressed proteins in disease samples is expanding rapidly. However, in spite of the identification of many candidate biomarkers, the number of biomarker proteins successfully applied to drug development has been limited. The main difficulty is the lack of a methodology to comprehensively analyze the expression or function of many candidate proteins and to efficiently select potential biomarker proteins of interest. To circumvent this problem, an improved technology to efficiently screen the truly valuable proteins from a large number of candidates is desirable.

Monoclonal antibodies are extremely useful tools for the functional and distributional analysis of proteins [4–6]. For example, they can be applied to the specific detection and study of proteins through various techniques including ELISA, Western blotting, fluorescent imaging and tissue microarray analysis (TMA). Of all these techniques, TMA is particularly valuable because it enables the analysis of clinical expression profiles of antigens from many clinical samples [7–11]. However, the common hybridoma-based antibody production is a laborious and time-consuming method. Thus, it is impractical to create antibodies against many differentially expressed proteins identified by proteomics technologies, such as two-dimensional differential in-gel electrophoresis (2D-DIGE) [12–15]. Furthermore, a relatively large amount of antigen (several milligrams) is necessary to produce an antibody (i.e., immunization of animals or screening of positive clones). The

* Corresponding author. Laboratory of Biopharmaceutical Research, National Institute of Biomedical Innovation, 7-6-8 Saito-Asagi, Ibaraki, Osaka 567-0085, Japan. Tel.: +81 72 641 9814; fax: +81 72 641 9817.
E-mail address: tsunoda@nibio.go.jp (S.-i. Tsunoda).
[1] These authors contributed equally to the work.

0142-9612/$ – see front matter © 2010 Elsevier Ltd. All rights reserved.
doi:10.1016/j.biomaterials.2010.09.030

production of protein on this scale often requires engineering the corresponding gene for heterologous expression, which may require some time to optimize. In this respect, phage antibody library technology is able to construct a large repertoire protein or peptide consisting of hundreds of millions of molecules. Monoclonal antibodies against target antigens are then rapidly obtained from the phage libraries displaying single chain fragment variable (scFv) antibodies *in vitro* [16–21].

However, the amount of protein in spots detected by 2D-DIGE analysis is generally very small (hundreds of nanograms). Therefore, a technology for generating monoclonal antibodies from such small amounts of antigen needs to be developed. There are no reports that describe the successful isolation of antibodies against small amounts of proteins obtained from differential proteome analysis.

Here, we report the establishment of a method for the efficient isolation of scFv antibody-expressing phages from a small amount of protein antigen prepared *via* 2D-DIGE spots using a high quality non-immune mouse scFv phage library [22]. We also describe an efficient method for screening and validating tumor-related biomarker proteins of interest from a number of differentially expressed proteins by expression profiling using TMA and scFv antibody-expressing phages.

2. Materials and methods

2.1. Non-immune mouse scFv phage library

Construction of the improved non-immune murine scFv phage library has been described previously [22]. The phage library was prepared from a TG1 glycerol stock containing the scFv gene library.

2.2. Affinity panning using BIAcore® and nitrocellulose membrane

Three different amounts (5000 ng, 50 ng or 0.5 ng) of KDR-Fc chimera (R&D systems Inc., Minneapolis, MN) or a portion of the proteins (1–5 ng) extracted from 2D-DIGE spots were immobilized on a BIAcore sensor chip CM3® (BIAcore, Uppsala, Sweden) or on a nitrocellulose membrane. BIAcore-based panning has been described previously [22]. Membrane-based panning was performed using the Bio-Dot Microfiltration Apparatus (Bio-Rad Laboratories, Hercules, CA). The membrane was incubated with blocking solution (10% skimmed milk, 25% glycerol) for 2 h and then washed twice with 0.1% TBST (Tris-buffered saline containing 0.1% Tween 20). The model phage library (anti-KDR scFv antibody-expressing phages: wild type phage = 1: 100) or the non-immune scFv phage library was pre-incubated with 90% blocking solution at 4 °C for 1 h and then applied to each well. After 2–3 h incubation, the apparatus was washed ten times with TBST. Bound scFv antibody-expressing phages were then eluted with 100 mM triethylamine. The eluted phages were incubated in log phase *E. coli* TG1 cells and glycerol-stocks prepared for further repeat panning cycles. Phage titer was measured by counting the number of infected colony cells on Petrifilm (3M Co., St. Paul, MN).

2.3. Colony direct PCR

After the panning, colonies of phage-infected TG1 were picked up at random as PCR templates. The gene inserts of 16 clones were amplified by PCR using the following primers: primer-156 (5′-CAACGTGAAAAAATTATTATTCGC-3′) and primer-158 (5′-GTAAATGA ATTTTCTGTATGAGG-3′), which anneal to the sequences of pCANTAB5E phagemid vector (GE Healthcare Biosciences AB, Uppsala, Sweden). The size of insert DNA sequence was analyzed by agarose gel electrophoresis.

2.4. Cell lines

Human mammary gland cell line 184A1 (American Type Culture Collection; ATCC, Manassas, VA) was maintained by MEGM Bullet Kit (Takara Bio, Shiga, JAPAN). Mammary gland-derived breast cancer cell line SKBR3 (ATCC) was maintained in McCoy's 5a plus 10% FBS. All cells were grown at 37 °C in a humidified incubator with 5% CO_2.

2.5. 2D-DIGE analysis

Cell lysates were prepared from human mammary gland cell line 184A1 and mammary gland-derived breast cancer cell line SKBR3, and then solubilized with 7 M urea, 2 M thiourea, 4% CHAPS and 10 mM Tris–HCl (pH 8.5). The lysates were labeled at the ratio 50 μg protein: 400 pmol Cy3 or Cy5 protein labeling dye (GE Healthcare Biosciences AB) in dimethylformamide according to the manufacture's protocol. For first dimension separation, the labeled samples (each 50 μg) were combined and mixed with rehydration buffer (7 M urea, 2 M thiourea, 4% CHAPS, 2% DTT, 2% Pharmalyte (GE Healthcare Biosciences AB)) and applied to a 24-cm immobilized pH gradient gel strip (IPG-strip pH 5–6 NL). The samples for the spot-picking gel were prepared without labelling by Cy-dyes. For the second dimension separation, the IPG-strips were applied to SDS-PAGE gels (10% polyacrylamide and 2.7% N,N′-diallyltartardiamide gels). After electrophoresis, the gels were scanned with a laser fluoroimager (Typhoon Trio, GE Healthcare Biosciences AB). The spot-picking gel was scanned after staining with Flamingo solution (Bio-Rad). Quantitative analysis of protein spots was carried out with Decyder-DIA software (GE Healthcare Biosciences AB). For the antigen spots of interest, spots of 1 × 1 mm in size were picked using an Ettan Spot Picker (GE Healthcare Biosciences AB). Proteins were extracted by solubilizing the picked gel pieces using 88 mM sodium periodide. Protein volumes were determined by BSA standard in Colloid Gold Total Protein staining (Bio-Rad).

2.6. In-gel tryptic digestion

Spots of 1 mm × 1 mm in size were picked using an Ettan Spot Picker and digested with trypsin as described below. The gel pieces were then destained with 50% acetonitrile/50 mM NH_4HCO_3 for 20 min twice, dehydrated with 75% acetonitrile for 20 min, and then dried using a centrifugal concentrator. Next, 5 μl of 20 μl/ml trypsin (Promega, Madison, WI) solution was added to each gel piece and incubated for 16 h at 37 °C. Three solutions were used to extract the resulting peptide mixtures from the gel pieces. First, 50 μl of 50% (v/v) acetonitrile in 1% (v/v) aqueous trifluoroacetic acid (TFA) was added to the gel pieces, which were then sonicated for 5 min. Next, we collected the solution and added 80% (v/v) acetonitrile in 0.2% TFA. Finally, 100% acetonitrile was added for the last extraction. The peptides were dried and then resuspended in 10 μl of 0.1% TFA before being cleaned using ZipTip^{TM} μC_{18} pipette tips (Millipore, Billerica, MA). The tips were wetted with three washes in 50% acetonitrile and equilibrated with three washes in 0.1% TFA, then the peptides were aspirated 10 times to ensure binding to the column. The column and peptides were washed three times in 0.1% TFA before being eluted in 1 μl of 80% acetonitrile/0.2% TFA.

2.7. Mass spectrometry (MS) and database search

The tryptic digests (0.6 μl) were mixed with 0.6 μl α-cyano-4-hydroxy-trans-cinnamic acid saturated in a 0.1% TFA and acetonitrile solution (1:1vol/vol). Each mixture was deposited onto a well of a 96-well target plate and then analyzed by matrix-assisted laser desorption ionization time-of-flight mass spectrometry (MALDI-TOF/MS; autoflexII, Bruker Daltonics, Billerica, WI) in the Reflectron mode. The mass axis was adjusted with calibration peptide (BRUKER DALTNICS) peaks (M/z 1047.19, 1296.68, or 2465.19) as lock masses. Bioinformatic databases were searched to identify the proteins based on the tryptic fragment sizes. The Mascot search engine (http://www.matrixscience.com) was initially used to query the entire theoretical tryptic peptide as well as SwissProt (http://www.expasy.org/, a public domain database provided by the Swiss Institute of Bioinformatics, Geneva, Switzerland). The search query assumed the following: (i) the peptides were monoisotopic (ii) methionine residues may be oxidized (iii) all cysteines are modified with iodoacetamide.

2.8. Phage ELISA using nitrocellulose membrane

Phage ELISA using scFv antibody-expressing phages was performed as previously described [22]. Briefly, phage-infected TG1 clones were picked, monocloned in a Bio-Dot Microfiltration Apparatus and scFv antibody-expressing phages propagated. The supernatants containing scFv antibody-expressing phages were incubated with immobilized proteins (~1 ng) extracted from 2D-DIGE spots. scFv antibody-expressing phages bound to 2D-DIGE spots were visualized using HRP-conjugated anti-M13 monoclonal antibody (GE Healthcare Biosciences AB).

2.9. Immunohistochemical staining using scFv antibody-expressing phages

Human breast cancer and normal TMA (Super Bio Chips, Seoul, South Korea & Biomax, Rockville, MD) were deparaffinated in xylene and rehydrated in a graded series of ethanol. Heat-induced epitope retrieval was performed in while keeping Target Retrieval Solution pH 9 (Dako, Glostrup, Denmark) temperature following the manufacturer's instructions. Heat-induced epitope retrieval was performed while maintaining the Target Retrieval Solution pH 9 (Dako) at the desired temperature according to the manufacturer's instructions. After heat-induced epitope retrieval treatment, endogenous peroxidase was blocked with 0.3% H_2O_2 in TBS for 5 min followed by washing twice in TBS. TMA were incubated with 5% BSA blocking solution for 15 min. The slides were then incubated with the primary scFv antibody-expressing phages (10^{12} CFU/ml) for 60 min. After washing three times with 0.05% TBST, each series of sections was incubated for 30 min with ENVISION + Dual Link (Dako), washed three times in TBST. The reaction products were rinsed twice with TBST, and then developed in liquid 3,3′-diaminobenzidine (Dako) for 3 min. After the development, sections were washed twice with distilled water, lightly

counterstained with Mayer's hematoxylin, dehydrated, cleared, and mounted with resinous mounting medium. All procedures were performed using AutoStainer (Dako).

2.10. TMA Immunohistochemistry scoring

The optimized staining condition for breast tumor tissue microarray was determined based on the coexistence of both positive and negative cells in the same tissue sample. Signals were considered positive when reaction products were localized in the expected cellular component. The criteria for the staining were scored as follows: distribution score was scored as 0 (0%), 1 (1–50%), and 2 (51–100%) to indicate the percentage of positive cells in all tumor cells present in one tissue. The intensity of the signal (intensity score) was scored as 0 (no signal), 1 (weak), 2 (moderate) or 3 (marked). The total of the distribution score and intensity score was then summed into a total score (TS) of TS0 (sum = 0), TS1 (sum = 2), TS2 (sum = 3), and TS3 (sum = 4–5). Throughout this study, TS0 or TS1 was regarded as negative, whereas TS2 or TS3 was regarded as positive. Statview software was used in statistical analysis.

3. Results

3.1. Optimization of panning methods

To establish a method for the efficient isolation of antibodies against a small amount of protein antigen (nanogram-order or less) prepared from 2D-DIGE spots, 5000 ng, 50 ng or 0.5 ng of recombinant KDR proteins were first immobilized on a BIAcore sensor chip CM3® or on a nitrocellulose membrane using the Bio-Dot Microfiltration Apparatus®. Isolation of antibodies was assessed using a model phage library (anti-KDR scFv antibody-expressing phages: wild type phage = 1: 100) (Fig. 1). Enrichment of the desired clones in the output library was evaluated by analyzing the gene inserts of randomly-picked phage-infected TG1 cells by colony direct PCR. In the method using BIAcore®, enrichment was observed when 5000 ng of KDR was used for immobilization. By contrast, Membrane-based panning led to the successful enrichment of anti-KDR scFv antibodies from only 0.5 ng of KDR. These results demonstrated that membrane-based panning was suitable for the isolation of antibodies from very small amounts of antigen extracted from 2D-DIGE spot gel pieces.

3.2. 2D-DIGE analysis and identification of differentially expressed proteins

To identify breast tumor-related biomarker proteins and isolate monoclonal antibodies against them, we performed 2D-DIGE using breast cancer cell lines SKBR3 and normal breast cell lines 184A1 (Fig. 2). Quantitative analysis showed that 21 spots displayed increased or decreased expression levels in the cancer cell line compared with the normal cell line. MALDI-TOF/MS analysis of the spots subsequently identified 16 different proteins (Table 1).

3.3. Isolation of antibodies against each 2D-DIGE spot from the non-immune scFv phage library

The amount of protein extracted from the gel pieces ranged from several tens of nanogram to a few micrograms (Table 1). Because the membrane-based panning method facilitates the isolation of antibodies from 0.5 ng of protein (Fig. 1), we reasoned that this method could be used to isolate antibodies from the small amounts of proteins extracted from 2D-DIGE spot gel pieces. Thus a portion of the extracted proteins were immobilized onto nitrocellulose membranes by means of a Bio-Dot Microfiltration Apparatus, and membrane-based panning was performed using the non-immune scFv phage library [22] (Table 2). The results from this panning showed that the output/input ratio of phage titer (titer of the recovered phage library after the panning/titer of phage library before the panning) after the fourth round of panning against all spots increased approximately 20-fold–4000-fold in comparison to that obtained from the first round of panning. This elevated output/input ratio indicated the enrichment of the antigen-binding scFv antibody clones. To isolate monoclonal scFv antibodies to each spot, a total of 60 clones were randomly picked from the 4th panning output phage library and binding of the monoclonal scFv antibody-expressing phages to each antigen was tested by phage ELISA. As a result, several scFv antibody clones binding to each of the 16 antigens were isolated (Table 2). The antigenic specificity of isolated scFv antibodies was investigated by dot blot using various proteins as antigens. Some of the isolated scFv antibodies bound specifically to the antigen protein, but not to the His-tagged caspase-8, His-tagged importin-β, tumor necrosis factor receptor 1 (TNFR1)-Fc-chimera and KDR-Fc-chimera (data not shown). These results indicated the successful isolation of each spot-specific scFv antibody-expressing phages after only two weeks.

3.4. TMA analysis

The next stage in the process was to select the most valuable breast tumor-related biomarker proteins from a large number of

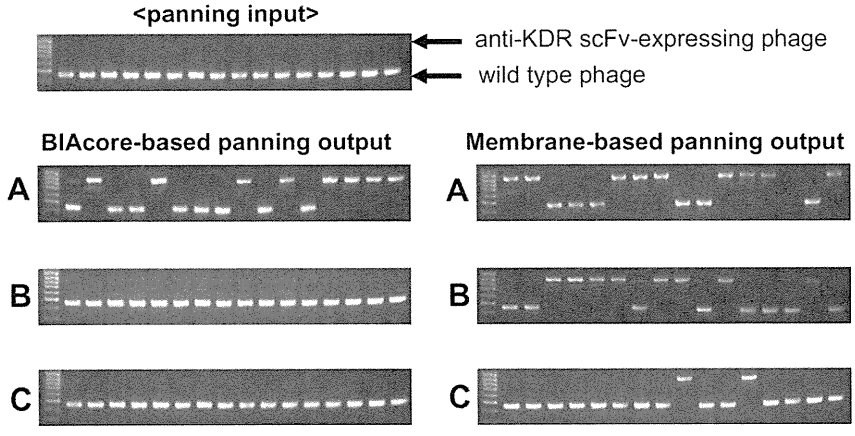

Fig. 1. Optimization of panning methods to isolate monoclonal antibodies from a very small amount of antigen. Model panning was performed using the BIAcore® or nitrocellulose membrane. The model library (anti-KDR scFv phage : wild type phage = 1: 100) was incubated with KDR ((A) 5000 ng, (B) 50 ng, (C) 0.5 ng) immobilized on a sensor chip or nitrocellulose membrane. The BIAcore-based panning method has been previously described [22]. After the binding step, the nitrocellulose membrane was washed ten times with TBST. The bound scFv antibody-expressing phages were eluted with triethylamine. The eluted scFv antibody-expressing phages were then incubated in log phase TG1 cells and individual TG1 clones were picked at random. Inserts of 16 phage clones were amplified by PCR. The gene sizes of inserts were analyzed by agarose gel electrophoresis.

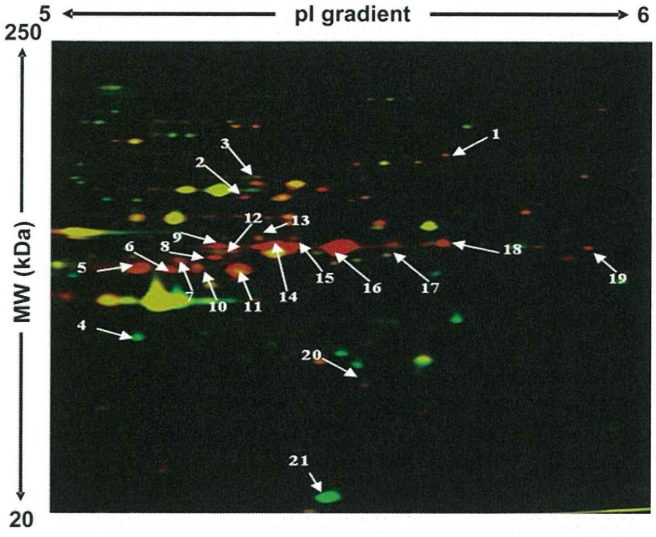

Fig. 2. 2D-DIGE image of fluorescently labeled proteins from SKBR3 and 184A cell. Breast cancer cell line (SKBR3) and normal breast cell line (184A1) were labeled using cy3 and cy5, respectively. The protein samples were then subjected to 2D electrophoresis. Spots that were over- and under-expressed in mammary cancer cells relative to normal cells were colored red and green, respectively. Yellow color spots show no change in expression.

identified candidate proteins. To this end, we immunostained TMA slides with 189 cases of breast tumors and 15 cases of normal breast specimens using the isolated spot-specific scFv antibody-expressing phages and screened the promising candidate biomarker proteins in terms of the expression profile in breast tumor tissues and normal tissues (Table 3). The result of the expression profile analysis showed that SPATA5, beta-actin variant, FLJ31438, PAK65, XRN1 and Jerky protein homolog-like were not expressed in normal and breast cancer tissue at all. By contrast, TRAIL-R2, Cytokeratin 8 and Eph receptor A10 were highly and specifically expressed (Fig. 3) in 63, 73 and 49% of breast tumor cases respectively, while the existing-breast cancer marker, Her-2, was expressed in 28% of breast tumor cases (Table 3). Thus, the relationship between the expression of each antigen and the Her-2 expression profile was analyzed. The level of expression of TRAIL-R2, Cytokeratin 8 and Eph receptor A10 in Her-2 positive cases were 77, 77 and 62%, and in Her-2 negative cases were 57, 67 and 44%, respectively (Table 4). Furthermore, the relationship between the expression of each antigen and clinical stage was analyzed in 187 of the 189 cases where all the clinical data was available. The level of expression of Cytokeratin 8 and Eph receptor A10 increased with progression of clinical symptoms (Table 5).

Table 1
Identification of 2D-DIGE spots by MALDI-TOF/MS.

Spot	Protein name	Accession number	MW (kDa)	pI	Protein volume (ng)	Expression ratio [cancer/normal] (fold)
#1	splicing factor YT521-B	Q96MU7	85	5.9	119	6
#2	IkappaBR	Q96HA7	63	5.5	104	6
#3	SPATA5	C9JT97	76	5.6	94	7
#4	skin aspartic protease	Q53RT3	37	5.3	610	0.1
#5	beta actin variant	P60709	42	5.3	99	15
#6	TRAIL-R2	O14763	48	5.4	100	18
#7	Cytokeratin-18	P05783	48	5.3	99	12
#8	TRAIL-R2	O14763	48	5.4	95	16
#9	RREB1	Q92766	52	5.3	109	10
#10	Cytokeratin-7	P08729	51	5.4	126	23
#11	Cytokeratin-18	P05783	48	5.3	497	13
#12	Cytokeratin-7	P08729	51	5.4	122	24
#13	FLJ31438	Q96N41	53	5.5	126	35
#14	Cytokeratin-7	P08729	51	5.4	406	36
#15	PAK65	Q13177	55	5.7	677	8
#16	Cytokeratin 8	P05787	54	5.5	694	32
#17	Cytokeratin 8	P05787	54	5.5	1143	72
#18	XRN1	Q8IZH2	54	5.8	353	8
#19	Jerky protein homolog-like	Q9Y4A0	51	6.0	130	22
#20	Eph receptor A10	Q5JZY3	32	5.7	119	9
#21	Glutathione S-transferase P	P09211	23	5.4	119	0.02

Table 2
Enrichment and isolation of antibodies to 2D-DIGE spots from non-immune libraries.

Spot	Protein name	Output/Input Ratio ($\times 10^{-7}$)/round				The number of isolated mAb.
		1st	2nd	3rd	4th	
#1	splicing factor YT521-B	6	7	16	480	4
#2	IkappaBR	6	7	15	500	3
#3	SPATA5	5	6	32	860	2
#4	skin aspartic protease	5	6	5	24	1
#5	beta actin variant	7	11	17	480	1
#6	TRAIL-R2	6	7	25	420	5
#7	Cytokeratin 18	5	11	62	260	4
#8	TRAIL-R2	5	27	41	1500	5
#9	RREB1	8	9	14	370	7
#10	Cytokeratin 7	6	7	3	2200	5
#11	Cytokeratin 18	6	8	15	84	2
#12	Cytokeratin 7	10	11	13	94	2
#13	FLJ31438	7	9	32	80	6
#14	Cytokeratin 7	4	7	46	280	5
#15	PAK65	7	11	51	580	9
#16	Cytokeratin 8	8	7	16	4100	6
#17	Cytokeratin 8	5	12	33	240	2
#18	XRN1	6	20	18	200	1
#19	Jerky protein homolog-like	7	10	49	940	3
#20	Eph receptor A10	8	6	57	3000	2
#21	Glutathione S-transferase P	7	8	110	1900	2

4. Discussion

Here, we aimed to develop a method of efficiently screening tumor-related biomarker proteins by proteome analysis. In

Table 3
Positive rate of identified proteins in breast cancer and normal breast tissues.

Protein name	Positive rate of antigens			
	Normal breast tissues		Breast cancer tissues	
Her-2	0/15	(0%)	53/189	(28%)
IkappaBR	3/15	(20%)	22/189	(12%)
SPATA5	0/15	(0%)	0/189	(0%)
beta actin variant	0/15	(0%)	0/189	(0%)
TRAIL-R2	0/15	(0%)	119/189	(63%)
RREB1	1/15	(7%)	83/189	(44%)
FLJ31438	0/15	(0%)	0/189	(0%)
PAK65	0/15	(0%)	0/189	(0%)
Cytokeratin 8	0/15	(0%)	137/189	(73%)
XRN1	0/15	(0%)	0/189	(0%)
Jerky protein homolog-like	0/15	(0%)	0/189	(0%)
Eph receptor A10	0/15	(0%)	93/189	(49%)

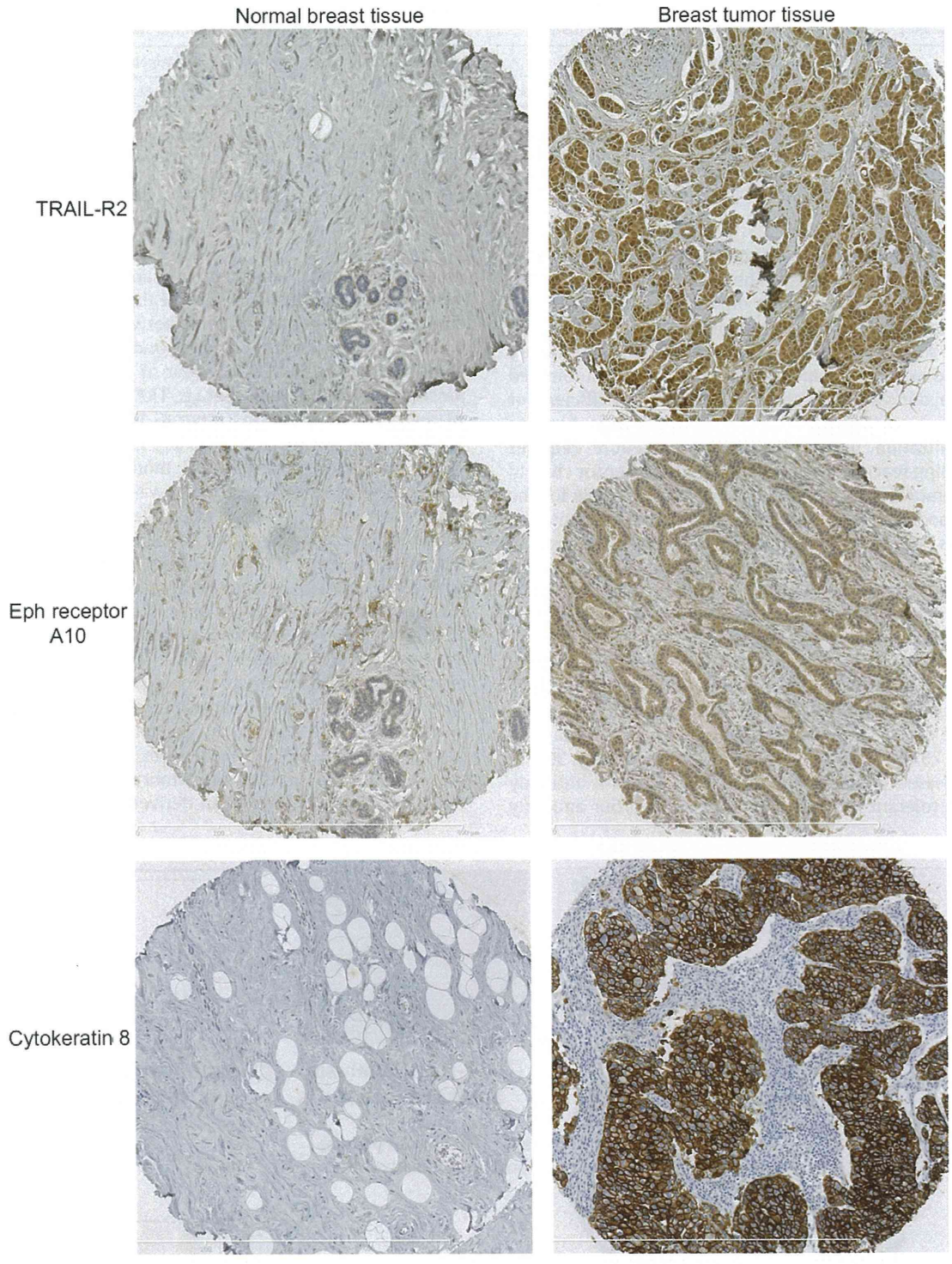

Fig. 3. Immunohistochemical staining of breast tumor and normal breast tissue microarray by scFv antibody-expressing phages. Typical images of breast cancer and normal breast tissue microarray stained by using scFv antibody-expressing phages to TRAIL-R2, Eph receptor A10 and Cytokeratin 8 are shown. Left panels are normal breast tissues and right panels are breast tumors. The tissue microarrays were counterstained by hematoxylin.

particular, we attempted to establish a means of isolating specific antibodies directly from small amounts of differentially expressed proteins obtained *via* 2D-DIGE analysis. To achieve this, we focused on a non-immune scFv phage library. Because the non-immune naïve scFv phage library has a huge repertoire of scFv on the surface of the phages, monoclonal antibodies to every antigen could be effectively isolated *in vitro*. Generally the diversity of the CDR3 domain, which is important for antigen-binding specificity, is estimated to be approximately twenty million [23]. Thus we reasoned that our previously constructed library, containing 2.4×10^9 scFv variants, has almost equal potential as the murine or human immune system [22]. Initially, in order to isolate monoclonal antibodies against very small amounts of antigen (hundreds of nanograms) recovered from the spots of 2D-DIGE analysis, we attempted to optimize the panning method using either a BIAcore® or nitrocellulose membrane. In the method using BIAcore®, the

Table 4
Positive rate of identified proteins in Her-2 positive and Her-2 negative cases.

Protein name	Positive rate of antigens in Her-2	
	Positive cases	Negative cases
TRAIL-R2	41/53 (77%)	78/136 (57%)
Cytokeratin 8	41/53 (77%)	91/136 (67%)
Eph receptor A10	33/53 (62%)	60/136 (44%)
TRAIL-R2 or Eph receptor A10	46/53 (87%)	100/136 (74%)

Table 5
Positive rate of identified proteins in clinical stage.

Protein name	Positive rate of antigens in clinical stage					
	Stage I		Stage II		Stage III	
Her-2	6/14	(43%)	17/87	(20%)	30/86	(35%)
TRAIL-R2	11/14	(79%)	51/87	(59%)	55/86	(64%)
Cytokeratin 8*	7/14	(50%)	58/87	(67%)	71/86	(83%)
Eph receptor A10*	4/14	(29%)	42/87	(48%)	47/86	(55%)
			Man Whitney U test $^*P < 0.05$			

enrichment of the desired clones was observed when immobilizing 5000 ng of KDR. By contrast, membrane-based panning led to the successful enrichment of clones from only 0.5 ng of KDR (Fig. 1). BIAcore-based panning has been recognized to be an effective method because the interaction of an antigen and a scFv antibody can be monitored in real time and the operation can be automated [24,25]. However, our results suggest that BIAcore® is inefficient for immobilizing very small amounts of antigen. This is because antigen immobilization using the BIAcore procedure requires a chemical coupling reaction with the surface of the sensor chip. In contrast, the membrane-based panning method is suitable for the isolation of antibodies against very small amounts of antigens. The suitability of this procedure when handling such small amounts of proteins presumably arises from the high efficiency of adsorption of antigens by the nitrocellulose membrane. These results show that monoclonal antibodies can be created from small amounts of proteins recovered from 2D-DIGE spots.

In breast cancer patients, the antibody targeting human epidermal growth factor receptor II (Her-2), is an effective drug [26,27]. However, because this receptor is over-expressed in only ~25% of breast cancer patients, anti-Her-2 antibody therapy is ineffective in ~75% of cases. Furthemore, approximately 30% of Her-2 over-expressed patients that received anti-Her-2 antibody therapy became tolerant [28–30]. Thus, we applied our antibody proteomics system to breast cancer samples for identification of the proteins to replace Her-2 as suitable therapeutic targets. Initially, 21 differentially expressed proteins between SKBR3 and 184A1 cells were found by 2D-DIGE analysis and 16 different proteins were identified by MALDI-TOF/MS. Four of the identified proteins were present in more than one spot i.e., TRAIL-R2 (spot 6, 8), Cytokeratin 18 (spot 7, 11), Cytokeratin 8 (spot 16, 17) and Cytokeratin 7 (spot 10, 12, 14). These proteins presumably display different pI and MW values due to posttranslational modification. Next, membrane-based panning against these spots was performed, and the output/input ratio of phage titer after the fourth round of panning increased from approximately 20-fold–4000-fold in comparison to that after the first round of panning. Moreover, we screened scFv antibody-expressing phages binding to each spot protein by phage ELISA and obtained each spot-specific scFv antibodies from all spots after approximately two weeks. Finally, it was necessary to select the most valuable proteins from a large number of differentially expressed proteins in breast cancer cells. Using the isolated spot-specific scFv antibody-expressing phages, we immunostained a TMA with 189 cases of breast cancer tissue and 15 samples of normal tissue. SPATA5, Beta actin, FLJ31438, PAK65 and XRN1 were not detected in either the tumor tissue or normal tissue. Thus, these proteins may have been derived from cell lines used in the

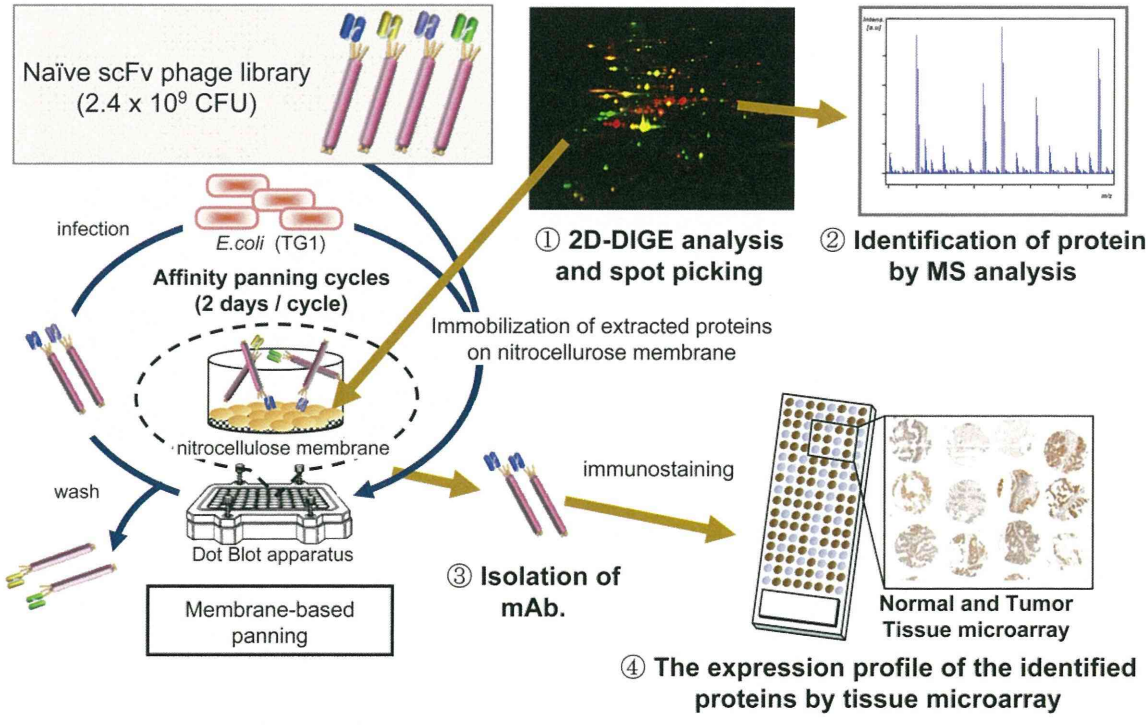

Fig. 4. Schematic illustration of the antibody proteomics system. Antibody proteomics system is an efficient method for screening tumor-related biomarker proteins. Because this system involves the direct isolation of monoclonal antibodies from 2D-DIGE spots without preparation of recombinant proteins, it enables the discovery and validation of tumor-related biomarker proteins by TMA analysis using the isolated scFv antibody-expressing phages.

proteome analysis or the antibodies against these proteins may not detect the antigen on formalin-fixed paraffin-embedded tissues. By contrast, TRAIL-R2, Cytokeratin 8 and Eph receptor A10 were specifically-expressed in over 40% of breast cancer tissues. We confirmed the immunohistochemical staining image generated by scFv antibody-expressing phages displayed a similar pattern to that generated by IgG type commercial antibody (data not shown). Interestingly, the expression rates of TRAIL-R2, Cytokeratin 8 and Eph receptor A10 were higher than the existing breast cancer marker, Her-2 (only about 25%). Moreover, the expression rates of TRAIL-R2 and Eph receptor A10 (cell membrane proteins) in Her-2 negative cases were over 40% and in Her-2 positive cases over 60%. This data indicates that TRAIL-R2 and Eph receptor A10 are promising alternative target candidates for anti-Her-2 antibody therapy ineffective patients, at least in terms of the expression profile. Further work is required to analyze the function of these proteins in more detail. Furthermore, by checking antigen expression profiles against clinical information, the expression rate of Cytokeratin 8 and Eph receptor A10 was found to have increased during progression of the clinical symptoms. These observations indicate that Cytokeratin 8 and Eph receptor A10 are promising diagnostic marker candidates for assessing the aggressiveness of breast cancer.

Recently, an anti-TRAIL-R2 antibody has been developed as an anticancer drug [31–33]. Moreover, Cytokeratin 8 has gained considerable attention as a cancer aggressiveness diagnostic marker [34–36]. These results demonstrate that this technology is able to select well-known drug-target markers (i.e., TRAIL-R2) and diagnostic markers (i.e., Cytokeratin 8) as well as unknown biomarker protein candidates (Eph receptor A10) from a large variety of differentially expressed proteins in cancer cells.

Our method employs a set of techniques for efficiently identifying biomarker candidates. Specifically, the method entails; 1) searching for differentially expressed proteins in disease samples, 2) identification of the proteins, 3) high throughput isolation of monoclonal antibodies against the proteins using a naïve scFv phage library, and 4) validation of the proteins by TMA analysis. This methodology is referred to as an "antibody proteomics system" (Fig. 4). We believe that the proteins identified using this approach will contribute to the drug development process. Indeed, the antibody proteomics system could become a platform technology for seeking tumor-related biomarker proteins by a proteomics-based approach.

5. Conclusions

In this study, we established the antibody proteomics system for efficiently screening and validating tumor-related biomarker proteins of interest by isolating specific antibodies directly from small amounts of proteins obtained *via* 2D-DIGE analysis. Applying this technique to the identification of breast tumor-related biomarker proteins, the expressions of Eph receptor A10, TRAIL-R2 and Cytokeratin 8 in breast tumor tissues were successfully validated from a large number of candidates. These results demonstrate that our original technology is an efficient and useful method for screening tumor-related biomarker proteins. Moreover, Eph receptor A10, TRAIL-R2 and Cytokeratin 8 identified in this study are promising breast tumor biomarkers for drug development.

Acknowledgement

We thank Dr. Junya Fukuoka, Department of Surgical Pathology, Toyama University Hospital, for valuable advice during our pathological analysis.

This study was supported in part by Grants-in-Aid for Scientific Research from the Ministry of Education, Culture, Sports, Science and Technology of Japan, and from the Japan Society for the Promotion of Science (JSPS). This study was also supported in part by Health Labour Sciences Research Grants from the Ministry of Health, Labor and Welfare of Japan, and by Health Sciences Research Grants for Research on Publicly Essential Drugs and Medical Devices from the Japan Health Sciences Foundation.

Appendix

Figure with essential color discrimination. Figs. 2–4 in this article have parts that are difficult to interpret in black and white. The full color images can be found in the on-line version, at doi:10.1016/j.biomaterials.2010.09.030.

References

[1] Hanash S. Disease proteomics. Nature 2003;422(6928):226–32.
[2] Kavallaris M, Marshall GM. Proteomics and disease: opportunities and challenges. Med J Aust 2005;182(11):575–9.
[3] Oh-Ishi M, Maeda T. Disease proteomics of high-molecular-mass proteins by two-dimensional gel electrophoresis with agarose gels in the first dimension (Agarose 2-DE). J Chromatogr B Analyt Technol Biomed Life Sci 2007;849 (1–2):211–22.
[4] Chaga GS. Antibody arrays for determination of relative protein abundances. Methods Mol Biol 2008;441:129–51.
[5] Kaufmann H, Bailey JE, Fussenegger M. Use of antibodies for detection of phosphorylated proteins separated by two-dimensional gel electrophoresis. Proteomics 2001;1(2):194–9.
[6] Xu ZW, Zhang T, Song CJ, Li Q, Zhuang R, Yang K, et al. Application of sandwich ELISA for detecting tag fusion proteins in high throughput. Appl Microbiol Biotechnol 2008;81(1):183–9.
[7] Au NH, Gown AM, Cheang M, Huntsman D, Yorida E, Elliott WM, et al. P63 expression in lung carcinoma: a tissue microarray study of 408 cases. Appl Immunohistochem Mol Morphol 2004;12(3):240–7.
[8] de Jong D, Xie W, Rosenwald A, Chhanabhai M, Gaulard P, Klapper W, et al. Immunohistochemical prognostic markers in diffuse large B-cell lymphoma: validation of tissue microarray as a prerequisite for broad clinical applications (a study from the Lunenburg Lymphoma Biomarker Consortium). J Clin Pathol 2009;62(2):128–38.
[9] Kozarova A, Petrinac S, Ali A, Hudson JW. Array of informatics: applications in modern research. J Proteome Res 2006;5(5):1051–9.
[10] Rimm DL, Camp RL, Charette LA, Costa J, Olsen DA, Reiss M. Tissue microarray: a new technology for amplification of tissue resources. Cancer J 2001;7 (1):24–31.
[11] Tawfik El-Mansi M, Williams AR. Validation of tissue microarray technology using cervical adenocarcinoma and its precursors as a model system. Int J Gynecol Cancer 2006;16(3):1225–33.
[12] Asadi A, Pourfathollah AA, Mahdavi M, Eftekharian MM, Moazzeni SM. Preparation of antibody against horseradish peroxidase using hybridoma technology. Hum Antibodies 2008;17(3–4):73–8.
[13] Hadas E, Theilen G. Production of monoclonal antibodies. The effect of hybridoma concentration on the yield of antibody-producing clones. J Immunol Methods 1987;96(1):3–6.
[14] Makonkawkeyoon L, Pharephan S, Makonkawkeyoon S. Production of a mouse hybridoma secreting monoclonal antibody highly specific to hemoglobin Bart's (gamma4). Lab Hematol 2006;12(4):193–200.
[15] McKinney KL, Dilwith R, Belfort G. Optimizing antibody production in batch hybridoma cell culture. J Biotechnol 1995;40(1):31–48.
[16] Barbas 3rd CF, Kang AS, Lerner RA, Benkovic SJ. Assembly of combinatorial antibody libraries on phage surfaces: the gene III site. Proc Natl Acad Sci U S A 1991;88(18):7978–82.
[17] Coomber DW. Panning of antibody phage-display libraries. Standard protocols. Methods Mol Biol 2002;178:133–45.
[18] McCafferty J, Griffiths AD, Winter G, Chiswell DJ. Phage antibodies: filamentous phage displaying antibody variable domains. Nature 1990;348 (6301):552–4.
[19] Okamoto T, Mukai Y, Yoshioka Y, Shibata H, Kawamura M, Yamamoto Y, et al. Optimal construction of non-immune scFv phage display libraries from mouse bone marrow and spleen established to select specific scFvs efficiently binding to antigen. Biochem Biophys Res Commun 2004;323 (2):583–91.
[20] Smith GP. Filamentous fusion phage: novel expression vectors that display cloned antigens on the virion surface. Science 1985;228(4705):1315–7.
[21] Vaughan TJ, Williams AJ, Pritchard K, Osbourn JK, Pope AR, Earnshaw JC, et al. Human antibodies with sub-nanomolar affinities isolated from a large non-immunized phage display library. Nat Biotechnol 1996;14(3):309–14.

[22] Imai S, Mukai Y, Nagano K, Shibata H, Sugita T, Abe Y, et al. Quality enhancement of the non-immune phage scFv library to isolate effective antibodies. Biol Pharm Bull 2006;29(7):1325–30.
[23] Xu JL, Davis MM. Diversity in the CDR3 region of V(H) is sufficient for most antibody specificities. Immunity 2000;13(1):37–45.
[24] Schier R, Marks JD. Efficient in vitro affinity maturation of phage antibodies using BIAcore guided selections. Hum Antibodies Hybridomas 1996;7 (3):97–105.
[25] Sheets MD, Amersdorfer P, Finnern R, Sargent P, Lindquist E, Schier R, et al. Efficient construction of a large nonimmune phage antibody library: the production of high-affinity human single-chain antibodies to protein antigens. Proc Natl Acad Sci U S A 1998;95(11):6157–62.
[26] Baselga J, Norton L, Albanell J, Kim YM, Mendelsohn J. Recombinant humanized anti-HER2 antibody (Herceptin) enhances the antitumor activity of paclitaxel and doxorubicin against HER2/neu overexpressing human breast cancer xenografts. Cancer Res 1998;58(13):2825–31.
[27] Pietras RJ, Pegram MD, Finn RS, Maneval DA, Slamon DJ. Remission of human breast cancer xenografts on therapy with humanized monoclonal antibody to HER-2 receptor and DNA-reactive drugs. Oncogene 1998;17(17):2235–49.
[28] Amar S, Moreno-Aspitia A, Perez EA. Issues and controversies in the treatment of HER2 positive metastatic breast cancer. Breast Cancer Res Treat 2008;109(1):1–7.
[29] Nahta R, Esteva FJ. In vitro effects of trastuzumab and vinorelbine in trastuzumab-resistant breast cancer cells. Cancer Chemother Pharmacol 2004;53 (2):186–90.
[30] Nahta R, Yu D, Hung MC, Hortobagyi GN, Esteva FJ. Mechanisms of disease: understanding resistance to HER2-targeted therapy in human breast cancer. Nat Clin Pract Oncol 2006;3(5):269–80.
[31] Plummer R, Attard G, Pacey S, Li L, Razak A, Perrett R, et al. Phase 1 and pharmacokinetic study of lexatumumab in patients with advanced cancers. Clin Cancer Res 2007;13(20):6187–94.
[32] Tolcher AW, Mita M, Meropol NJ, von Mehren M, Patnaik A, Padavic K, et al. Phase I pharmacokinetic and biologic correlative study of mapatumumab, a fully human monoclonal antibody with agonist activity to tumor necrosis factor-related apoptosis-inducing ligand receptor-1. J Clin Oncol 2007;25 (11):1390–5.
[33] Vannucchi S, Chiantore MV, Fiorucci G, Percario ZA, Leone S, Affabris E, et al. TRAIL is a key target in S-phase slowing-dependent apoptosis induced by interferon-beta in cervical carcinoma cells. Oncogene 2005;24(15):2536–46.
[34] Ditzel HJ, Strik MC, Larsen MK, Willis AC, Waseem A, Kejling K, et al. Cancer-associated cleavage of cytokeratin 8/18 heterotypic complexes exposes a neoepitope in human adenocarcinomas. J Biol Chem 2002;277 (24):21712–22.
[35] Fukunaga Y, Bandoh S, Fujita J, Yang Y, Ueda Y, Hojo S, et al. Expression of cytokeratin 8 in lung cancer cell lines and measurement of serum cytokeratin 8 in lung cancer patients. Lung Cancer 2002;38(1):31–8.
[36] Wolff JM, Borchers H, Brehmer Jr B, Brauers A, Jakse G. Cytokeratin 8/18 levels in patients with prostate cancer and benign prostatic hyperplasia. Urol Int 1998;60(3):152–5.

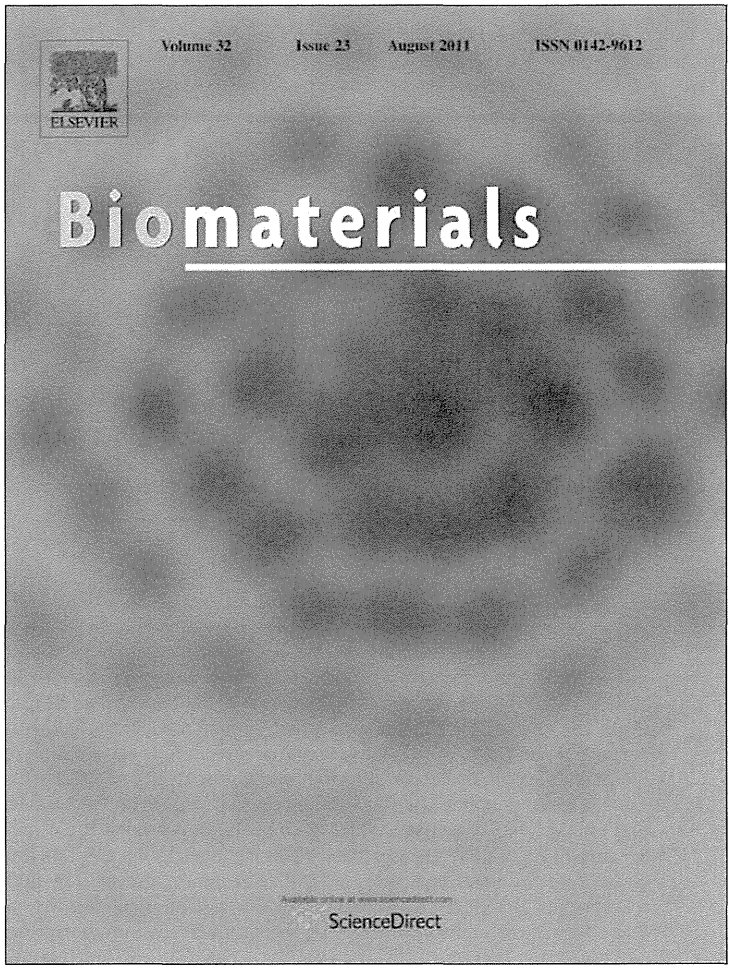

Biomaterials 32 (2011) 5498–5504

Contents lists available at ScienceDirect

Biomaterials

journal homepage: www.elsevier.com/locate/biomaterials

Fine tuning of receptor-selectivity for tumor necrosis factor-α using a phage display system with one-step competitive panning

Yasuhiro Abe [a], Tomoaki Yoshikawa [a,b], Masaki Inoue [a], Tetsuya Nomura [a], Takeshi Furuya [a,b], Takuya Yamashita [a,b], Kazuya Nagano [a], Hiromi Nabeshi [a,b], Yasuo Yoshioka [a,c], Yohei Mukai [a,b], Shinsaku Nakagawa [b,c], Haruhiko Kamada [a,c], Yasuo Tsutsumi [a,b,c], Shin-ichi Tsunoda [a,b,c,*]

[a] Laboratory of Biopharmaceutical Research, National Institute of Biomedical Innovation, 7-6-8 Saito-Asagi, Ibaraki, Osaka 567-0085, Japan
[b] Graduate School of Pharmaceutical Sciences, Osaka University, 1-6 Yamadaoka, Suita, Osaka 565-0871, Japan
[c] The Center of Advanced Medical Engineering and informatics, Osaka University, 1-6 Yamadaoka, Suita, Osaka 565-0871, Japan

ARTICLE INFO

Article history:
Received 24 March 2011
Accepted 5 April 2011
Available online 5 May 2011

Keywords:
Cytokine
Molecular biology
Protein
Affinity
Bioactivity

ABSTRACT

Tumor necrosis factor-α (TNF) is one of the attractive targets for the development of anti-inflammatory and anti-tumor drugs, because it is an important mediator in the pathogenesis of several inflammatory diseases and tumor progression. Thus, there is an increasing need to understand the TNF receptor (TNFR1 and TNFR2) biology for the development of TNFR-selective drugs. Nonetheless, the role of TNFRs, especially that of TNFR2, remains poorly understood. Here, using a unique competitive panning, we optimized our phage display-based screening technique for isolating receptor-selective TNF mutants, and identified several TNFR2-specific TNF mutants with high TNFR2 affinity and full bioactivity via TNFR2. Among these mutants, the R2-7 clone revealed very high TNFR2-selectivity (1.8×10^5 fold higher than that for the wild-type TNF), which is so far highest among the reported TNFR2-selective TNF mutants. Because of its high TNFR2-selectivity and full bioactivity, the TNF mutant R2-7 would not only help in elucidating the functional role of TNFR2 but would also help in understanding the structure-function relationship of TNF/TNFR2. In summary, our one-step competitive panning system is a simple, useful and effective technology for isolating receptor-selective mutant proteins.

1. Introduction

Tumor necrosis factor-α (TNF) is a major inflammatory cytokine that plays a central role in host defense and inflammation via two receptor subtypes, TNF receptor (TNFR)1 and TNFR2 [1,2]. Elevated serum levels of TNF correlates with the severity and progression of the inflammatory diseases such as rheumatoid arthritis (RA), inflammatory bowel disease, septic shock, multiple sclerosis and hepatitis [3–5]. Currently, TNF-neutralization therapies have proven successful for the treatment of RA [4,6,7]. However, these therapies can cause serious side effects, such as tuberculosis, because TNF-dependent host defense functions are also inhibited [8,9]. Therefore, understanding the function of TNF/TNFRs is important for optimal therapy of various TNF-related autoimmune diseases. TNFR1 is constitutively expressed in most tissues and seems to be the key mediator of TNF signaling [10,11]. In contrast, the expression of TNFR2 is more restricted and is found mainly on certain T-cell subpopulations [12], endothelial cells, cardiac myocytes [13] and neuronal tissue [14,15]. Recent studies suggested that TNFR2 signaling is associated with T-cell survival [16], cardioprotection [17,18], remyelination [19], and survival of some neuron subtypes [20,21]. Although the two TNFRs have been shown to have distinct functions in some cells [22], the physiological significance of the presence of both receptors is not fully understood. Especially TNFR2-induced signaling remains elusive and need further investigation.

In order to understand the mechanism of TNFRs, we have investigated the relationship between the biological activities and structural properties of a large number of TNF mutants by phage-display technique [23,24]. However, screening efficiency of isolating TNFR2-selective TNF mutants using this technique is extremely low, and it is difficult to prepare large repertoire of TNFR2-selective TNF mutants for the structure-activity relationship study. In our previous study, we screened 500 phage clones

* Corresponding author. Laboratory of Biopharmaceutical Research, National Institute of Biomedical Innovation, 7-6-8 Saito-Asagi, Ibaraki, Osaka 567-0085, Japan. Tel.: +81 72 641 9814; fax: +81 72 6419817.
E-mail address: tsunoda@nibio.go.jp (S.-i. Tsunoda).

0142-9612/$ – see front matter © 2011 Elsevier Ltd. All rights reserved.
doi:10.1016/j.biomaterials.2011.04.018

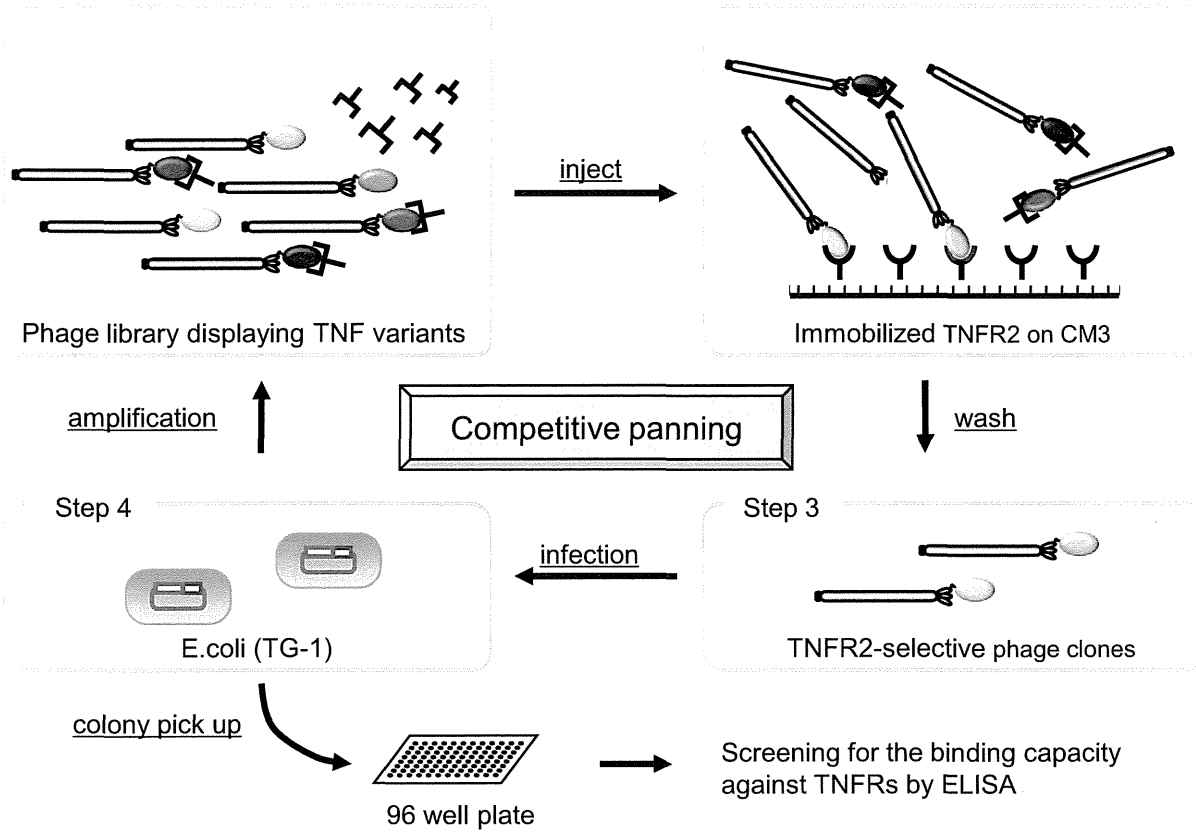

Fig. 1. Screening scheme for isolating TNFR2-selective TNF mutants using competitive panning. To concentrate TNFR2-selective mutant TNFs, phage libraries were pre-incubated with TNFR1 Fc chimera (TNFR1-Fc), and subsequent biopanning against the TNFR2 was carried out in the presence of TNFR1-Fc using the BIAcore biosensor. After several rounds of panning, phage clones were isolated and screened by ELISA.

for isolating TNFR2-selective mutants using the conventional panning method [23]. Out of the 500 clones, only 2 clones showed selectivity for TNFR2 binding that was 10-times higher than the wild-type TNF (wtTNF). Furthermore, bioactivities of these two TNFR2 selective TNF mutants were lower than that of wtTNF (<30%). To improve the screening efficacy, we optimized our phage display-based cytokine mutagenesis technology [25] with an unique competitive panning technique for identifying TNFR2-specific TNF mutants with higher affinity and bioactivity. In this competitive panning technique, phage libraries were pre-incubated with TNFR1 Fc chimera (TNFR1-Fc), and subsequent biopanning against the TNFR2 was carried out in the presence of TNFR1-Fc using the BIAcore biosensor. Since TNFR1-binding clones could not bind to TNFR2 due to steric hindrance, TNF mutants binding only to TNFR2 were selectively enriched with high efficiency. Using this optimized competitive panning technique, we have identified TNFR2-selective TNF mutants with full bioactivity via TNFR2.

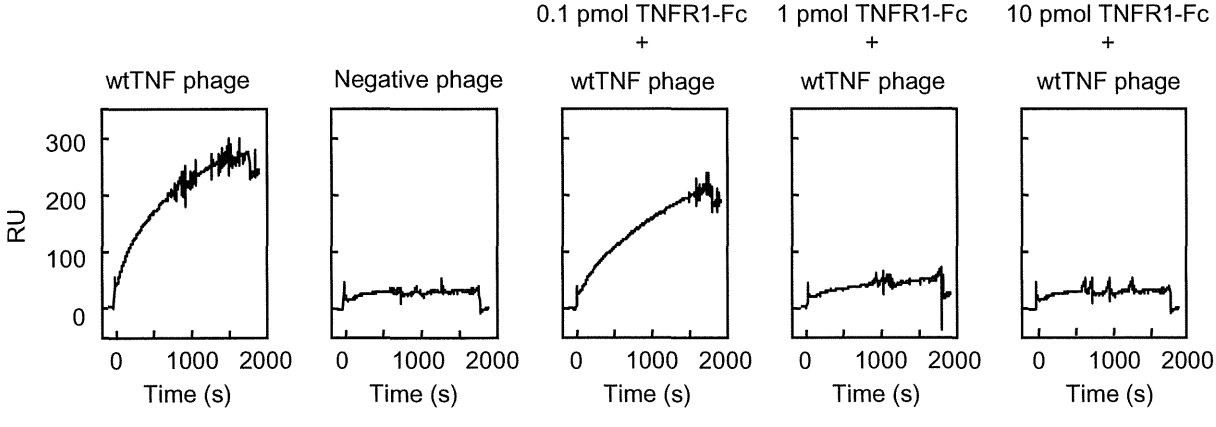

Fig. 2. Optimization of competitive panning using BIAcore biosensor. 0.1 pmol, 1 pmol or 10 pmol of human TNFR1-Fc was mixed with 1×10^{10} CFU phages displaying wtTNF for 2 h at 4 °C, and the mixture was passed over the TNFR2-immobilized CM3 sensor chip and real-time biomolecular interaction analyses were performed with BIAcore biosensor. Anti-CD25 single chain Fv-displaying phage was used as a negative control.

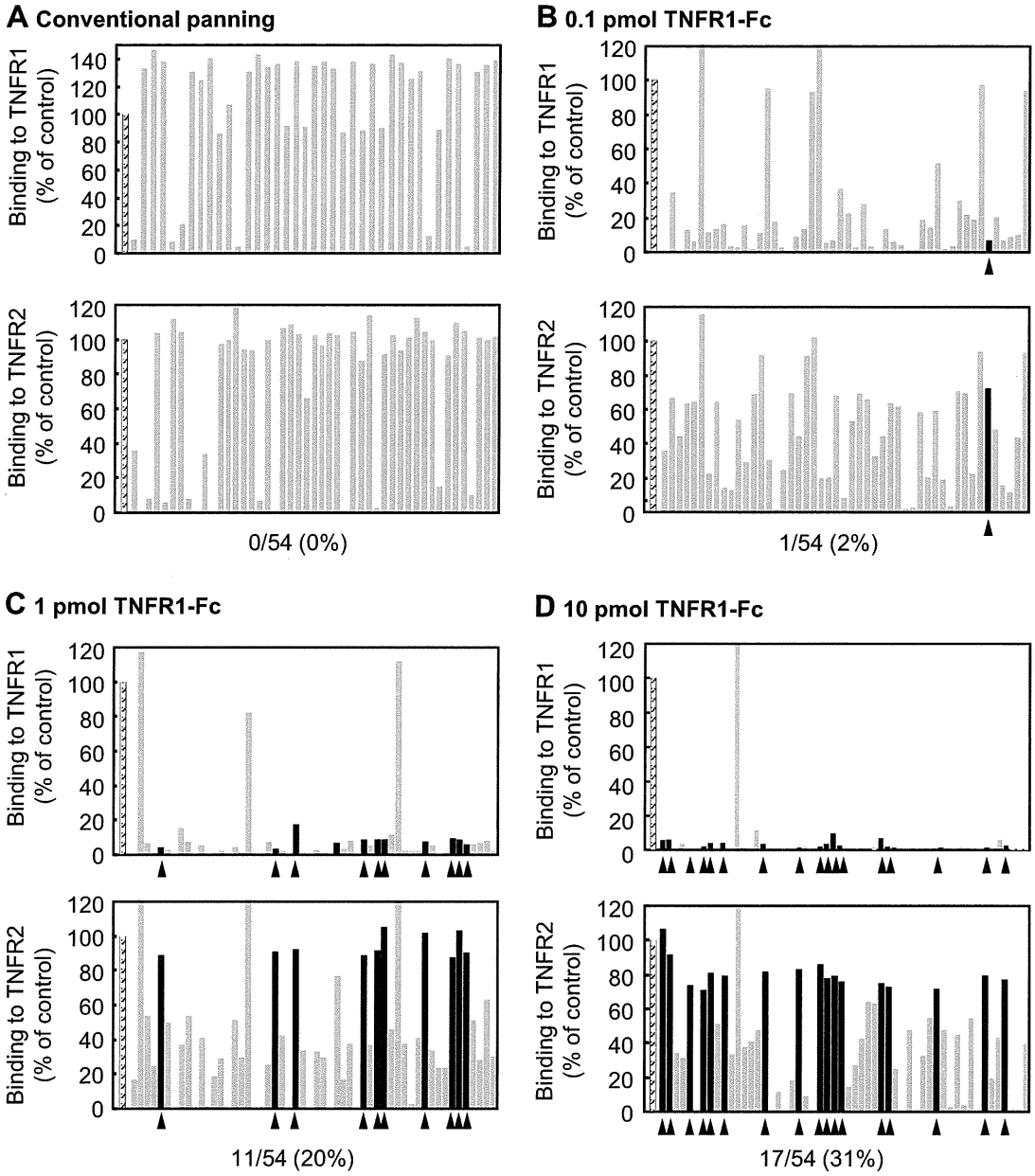

Fig. 3. Determination of relative affinities of mutant TNFs for TNFR1 or TNFR2 by capture ELISA. *E. coli* supernatant containing a TNF mutant (gray bar) from each panning conditions, in which phages were premixed with (A) none, (B) 0.1 pmol, (C) 1 pmol and (D) 10 pmol of TNFR1-Fc, were applied to the TNFR1-Fc or TNFR2-Fc immobilized plate and detected with biotinylated polyclonal anti-TNF antibody. wtTNF was used as a positive control (hatched bar). Affinities of TNFR2-selective clones (black bar) for TNFR2 was more than 70% of that of the wtTNF, and that for TNFR1 was less than 30% of that of the wtTNF.

2. Materials and methods

2.1. Cells

HEp-2 cells, a human fibroblast cell line, were provided by Cell Resource Center for Biomedical Research (Tohoku University, Sendai, Japan) and were maintained in RPMI 1640 (Sigma–Aldrich Japan, Tokyo, Japan) supplemented with 10% bovine fetal serum (FBS) 1 mM sodium pyruvate, 50 mM 2-mercaptoethanol, and antibiotics. hTNFR2/mFas-PA cells are preadipocytes derived from TNFR1$^{-/-}$R2$^{-/-}$ mice expressing a chimeric receptor, the extracellular and transmembrane domain of human TNFR2, and intracellular domain of mouse Fas; these cells were cultured in RPMI 1640 supplemented with 10% FBS, 5 μg/ml Blasticidin S HCl (Invitrogen, Carlsbad, CA), and antibiotics [26].

2.2. Library construction

Protocol for the construction of phage-display library displaying structural mutants of human TNF has been described previously [23]. In brief, multiple-mutations were introduced into the wtTNF gene by PCR to randomly replace the codons of 6 amino acid residues at positions 29, 31, 32, 145, 146 and 147, respectively, of the TNF protein. The PCR product was digested with the restriction enzymes Hind III and Not I, and ligated into the Hind III/Not I digested pY03′ phagemid vector for displaying the TNF mutants on the phage surface as g3p-fusion proteins.

2.3. Optimization of competitive panning using BIAcore biosensor

Human TNFR2-Fc (R&D systems, Minneapolis, MN) was diluted to 50 μg/ml in 10 mM sodium acetate buffer (pH 4.5) and immobilized onto a CM3 sensor chip using an amine coupling kit (GE Healthcare, UK), which resulted in an increase of 5000–6000 resonance units (RU). 0.1 pmol, 1 pmol or 10 pmol of human TNFR1-Fc (R&D systems) was mixed with 100 μl of wtTNF-displaying phage (1×10^{11} CFU/ml) for 2 h at 4 °C, and the mixture was passed over the TNFR2-immobilized CM3 sensor chip at a flow rate of 3 μl/min. The binding kinetics of the mixtures to TNFR2-Fc were analyzed by BIAcore 2000 (GE Healthcare).

Table 1
Amino acid sequences of wtTNF and TNFR2-selective TNF mutants.

Clone	Residue position					
	29	31	32	145	146	147
wtTNF	L	R	R	A	E	S
R2–6	L	R	R	H	E	D
R2–7	V	R	R	D	D	D
R2–8	L	R	R	N	D	D
R2–9	L	R	R	T	S	D
R2–10	L	R	R	Q	D	D
R2–11	L	R	R	T	D	D
R2–12	L	R	R	D	G	D
R2–13	L	R	R	D	E	D

2.4. Selection of phage displaying TNFR2-selective TNF mutants by competitive panning

1×10^{10} CFU phages displaying TNF mutants were pre-incubated for 2 h at 4 °C, with serially diluted TNFR1-Fc. The mixtures were injected at 3 μl/min over the sensor chip. After injection, the sensor chip was washed using the rinse command for 3 min. Elution was carried out using 20 μl of 10 mM glycine-HCl (pH 2.0) and the eluted phage was neutralized with 1 M Tris–HCl (pH 6.9). The recovered phages were amplified by infection of E. coli strain TG1 (Stratagene, La Jolla, CA), which allow read-through of the amber stop codon located between the TNF and g3p sequences of pY03′ phagemid vector. These steps were repeated twice. After final round of panning, the phage mixture was used to infect E. coli and plated on LB agar/ampicillin plates. Single clones of transfected TG1 were randomly picked from the plate and each colony was grown in 2-YT medium with ampicillin (100 μg/ml) and glucose (2% w/v) at 37 °C until the OD_{600} of the culture medium reached 0.4. Each culture was centrifuged, the supernatants were removed, and fresh 2-YT media with ampicillin (100 μg/ml) was added to each E. coli pellet. After incubation for 6 h at 37 °C supernatants were collected and used to determine affinity for TNFRs by capture ELISA as described previously [24]. After the procedure, the phagemid vectors were sequenced using a Big Dye Terminator v3.1 kit and ABI PRISM 3100 (Applied Biosystems Ltd., Pleasanton, CA).

2.5. Expression and purification of TNF mutants

Preparation of purified recombinant protein was described previously [25]. In brief, TNF mutants recombined into pYas1 vector, under the control of T7 promoter, were produced in E. coli (BL21λDE3). Mutant TNFs recovered from inclusion body, which were washed in Triton X-100 and solubilized in 6 M guanidine-HCl, 0.1 M Tris–HCl, pH 8.0, and 2 mM EDTA. Solubilized protein was adjusted to 10 mg/ml and was reduced with 10 mg/ml dithioerythritol for 4 h at RT and refolded by 100-fold dilution in a refolding buffer (100 mM Tris–HCl, 2 mM EDTA, 1 M arginine, and oxidized glutathione (551 mg/L)). After dialysis with 20 mM Tris–HCl, pH 7.4, containing 100 mM urea, active trimeric proteins were purified by Q-Sepharose (GE Healthcare)chromatography and size-exclusion chromatography (Superose 12; GE Healthcare).

2.6. Analysis of binding kinetics using surface plasmon resonance (SPR)

The binding kinetics of the wtTNF and TNF mutants were analyzed by the SPR technique (BIAcore 2000; GE Healthcare). TNFR1-Fc or TNFR2-Fc were separately immobilized on to CM5 sensor chip, resulting in an increase of 3000–3500 RU. During the association phase, wtTNF or TNF mutants diluted in running buffer (HBS-EP) at 156.8, 52.3, 17.4, 5.8 or 1.9 nM were passed over the immobilized TNFR2 for 2 min at a flow rate of 20 μl/min. During the dissociation phase, HBS-EP was run over the sensor chip for 1 min at a flow rate of 20 μl/min. The SPR measurements for TNFR1 were performed using much higher concentrations of TNF mutants (392.1, 130.7, 43.6, 14.5 or 4.8 nM). The data were analyzed globally with BIAevaluation 3.1 software (GE Healthcare) to apply a 1:1 Langmuir binding model. The obtained sensorgrams were fitted globally over the range of injected concentrations and simultaneously over the association and dissociation phages.

2.7. In vitro assessment of bioactivity via TNFR1 or TNFR2 with TNF mutants

HEp-2 cells were seeded at 4×10^4 cells/well in 96-well plates and incubated for 18 h with serially diluted wtTNF (Peprotech, Rocky Hill, NJ) or TNF mutants in the presence of 50 mg/ml cycloheximide. After incubation, cell survival was determined by methylene blue assay as described previously [25]. In the case of analyzing TNFR2-mediated biological activity, hTNFR2/mFas-PA were seeded on 96-well micro titer plates with a density of 1.5×10^4 cells/well in culture medium. Serial dilutions of wtTNF (Peprotech) and TNF mutants were prepared with 1 μg/ml cycloheximide and added to each well. After 48 h-incubation at 37 °C, the cell viabilities were analyzed using a WST-8 assay kit (Nacalai Tesque) according to the manufacturer's instructions.

3. Results

3.1. Optimization of one-step competitive panning protocol

To improve identifying TNFR2-selective TNF mutants with better bioactivity, we have introduced a step to remove the TNFR1-binding phages from the library by competitive panning using TNFR1-Fc. We postulated that TNFR1-binding clones could be eliminated when panning for the TNFR2-binding clones is performed in the presence of TNFR1 protein (see Fig. 1). Although an immunoplate or immunotube is commonly used for the panning [27–29], these techniques cannot make real-time observation of the interaction between phage library and receptor, and are difficult to automate and control the precise settings. Therefore, we first utilized the BIAcore biosensor and optimized the concentration of TNFR1-Fc required for eliminating the TNFR1-binding clones. Serially diluted human TNFR1-Fc was mixed with 1×10^{10} CFU phages displaying wtTNF, and the binding avidity of the phage-displayed wtTNF for TNFR2 was assessed using a BIAcore biosensor. As shown in Fig. 2, TNFR1-Fc inhibited the binding of phage-displayed wtTNF to TNFR2 in a dose-dependent manner. 10 pmol of TNFR1-Fc virtually abolished the binding of wtTNF not only to TNFR2 (last panel in Fig. 2) but also the binding of wtTNF to TNFR1 (data not shown). These results clearly suggest that 10 pmol of TNFR1-Fc would be sufficient for competitively subtract unwanted TNFR1-binding phage clones from a phage library displaying structural TNF mutants.

Table 2
Biding kinetics of TNFs to TNFR1 and TNFR2.

	TNFR1				TNFR2			
	k_{on}[a] (10^6 $M^{-1}s^{-1}$)	k_{off}[b] (10^{-4} s^{-1})	K_D[c] (10^{-10} M)	Relative[d] (%)	k_{on}[a] (10^6 $M^{-1}s^{-1}$)	k_{off}[b] (10^{-4} s^{-1})	K_D[c] (10^{-10} M)	Relative[d] (%)
wtTNF	0.45	1.3	2.9	100.0	2.0	12.1	6.1	100.0
R2–6	0.79	54.5	68.8	4.2	3.2	7.8	2.4	251.4
R2–7	0.44	116.0	262.0	1.1	2.1	7.4	3.6	169.7
R2–8	1.22	50.3	41.1	7.1	3.1	6.6	2.1	291.0
R2–9	1.19	50.1	42.3	6.9	3.8	12.6	3.3	185.2
R2–10	0.67	43.9	63.7	4.6	2.2	5.3	2.4	253.5
R2–11	0.81	87.5	108.	2.7	2.3	5.4	2.3	264.5
R2–12	1.36	98.8	72.6	4.0	4.1	10.6	2.6	235.0
R2–13	0.97	104.0	107.0	2.7	2.9	8.2	2.9	212.2

Kinetic parameters for each TNF were calculated from the respective sensorgram by BIAevaluation 3.1software, and taking into consideration that the TNF binds as a trimer.
[a] k_{on} is the association kinetic constant.
[b] k_{off} is the dissociation kinetic constant.
[c] K_D is the equilibrium dissociation constant ($K_D = k_{off}/k_{on}$).
[d] Relative values were calculated from the K_D (wtTNF)/K_D (TNF mutants) × 100.

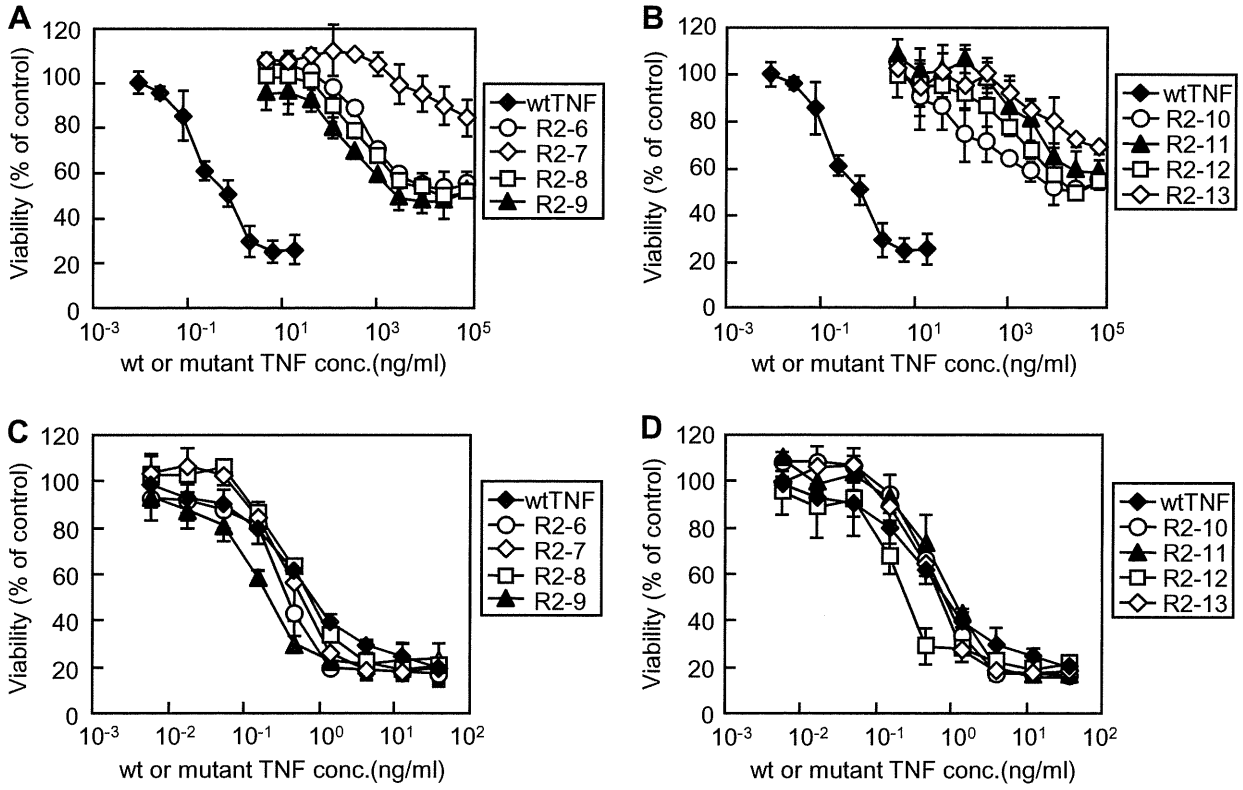

Fig. 4. In vitro bioactivity assay of TNF mutants via TNFR1 or TNFR2. The bioactivity of mutant TNFs via TNFR1 or TNFR2 were measured by cytotoxicity assay against HEp-2 cells (A and B) or hTNFR2/mFas-PA (C and D), respectively. Each point represents the mean ± S.D. of triplicate measurements.

3.2. Selection of TNFR2-selective TNF mutants by one-step competitive panning

To concentrate TNFR2-selective mutant TNFs, the TNF structural mutant displaying phage library was subjected to two rounds of conventional panning or competitive panning against TNFR2 using the BIAcore biosensor. After the second round of panning, *Escherichia coli* (TG1) supernatants of 54 randomly picked clones from each panning procedure were further screened by capture ELISA to analyze their binding specificities for each TNFR (Fig. 3). Consequently, we obtained numerous clones with high-affinity for TNFR2 under all panning conditions. Binding avidities of these clones for TNFR1 tended to decrease depending on the concentration of TNFR1-Fc used for premixing. However, binding avidity of a TNFR2-selective clone, which binds only to TNFR2 (Fig. 3, black bar), tended to increase depending on the concentration of TNFR1-Fc used for premixing. Almost all clones obtained from the conventional and competitive panning with 0.1 pmol of TNFR1-Fc (Fig. 3A and B, respectively) bound to TNFR1, and the panning efficiency for isolating the TNFR2-selective TNF mutants was <2%. In contrast, clones obtained from the subtracted panning with 1 or 10 pmol of TNFR1-Fc (Fig. 3C and D, respectively) contained many TNFR2-selective TNF mutants (>20%). From these panned clones, we eventually identified eight candidate agonists that selectively and strongly bound to the TNFR2. Amino acid sequences of these eight candidate TNFR2-selective TNF mutants are shown in Table 1. TNFR2-slective mutants were mutated near residue 145 and

Table 3
In vitro bioactivities of TNF mutants via TNFR1 or TNFR2.

	TNFR1[a]		TNFR2[b]		TNFR2/TNFR1[e]
	EC50[c] (ng/ml)	Relative Activity[d] (%)	EC50[c] (ng/ml)	Relative activity[d] (%)	
wtTNF	0.6	100	0.56	100	1.0
R2–6	8.1×10^3	7.3×10^{-3}	0.39	144	2.0×10^4
R2–7	$>1.0 \times 10^5$	$<6.0 \times 10^{-4}$	0.51	110	1.8×10^5
R2–8	4.6×10^3	1.2×10^{-2}	0.67	84	7.0×10^3
R2–9	2.1×10^3	2.8×10^{-2}	0.21	267	9.5×10^3
R2–10	1.1×10^4	5.4×10^{-3}	0.72	78	1.4×10^4
R2–11	6.7×10^4	8.9×10^{-4}	0.95	59	6.6×10^4
R2–12	2.6×10^4	2.2×10^{-3}	0.23	243	1.1×10^5
R2–13	$>1.0 \times 10^5$	$<6.0 \times 10^{-4}$	0.63	89	1.5×10^5

[a] Bioactivities of the wtTNF and TNF mutants via TNFR1 were measured by determining the TNF-induced cytotoxicity in HEp-2 cells.
[b] Bioactivities of the wtTNF and TNF mutants via TNFR2 were measured by determining the TNF-induced cytotoxicity in hTNFR2/mFas-PA.
[c] Experimental data were analyzed by a logistic regression model to calculate the mean effective concentration (EC50).
[d] Relative activities were calculated from the EC50 (wtTNF)/EC50 (TNF mutants).
[e] Selectivity for TNFR2 was calculated from the ratio of the relative activity (via TNFR2)/relative activity (via TNFR1).